Journal for ImmunoTherapy of Cancer

Allogeneic NK cells induce monocyte-to-dendritic cell conversion, control tumor growth, and trigger a pro-inflammatory shift in patient-derived cultures of primary and metastatic colorectal cancer

Elisa C Toffoli ,[1,2,3] Amanda A van Vliet ,[2,3,4,5] Henk W M Verheul,[6] Hans J van der Vliet,[1,2,7] Jurriaan Tuynman,[8] Jan Spanholtz,[4] Tanja D de Gruijl[1,2,3]

To cite: Toffoli EC, van Vliet AA, Verheul HWM, *et al*. Allogeneic NK cells induce monocyte-to-dendritic cell conversion, control tumor growth, and trigger a pro-inflammatory shift in patient-derived cultures of primary and metastatic colorectal cancer. *Journal for ImmunoTherapy of Cancer* 2023;**11**:e007554. doi:10.1136/jitc-2023-007554

► Additional supplemental material is published online only. To view, please visit the journal online (http://dx.doi.org/10.1136/jitc-2023-007554).

ECT and AAvV contributed equally.

Accepted 17 October 2023

For numbered affiliations see end of article.

Correspondence to
Professor Tanja D de Gruijl;
td.degruijl@amsterdamumc.nl

ABSTRACT

Introduction Natural killer (NK) cells are innate lymphocytes with a key role in the defense against tumors. Recently, allogeneic NK cell-based therapies have gained interest because of their ability to directly lyse tumor cells without inducing graft-versus-host disease. As NK cells are also able to influence the function of other immune cells (most notably dendritic cells (DC)), a better understanding of the effects of allogeneic NK cell products on the host immune system is required. In this study, we analyzed the effects of an allogeneic off-the-shelf NK cell product, on the tumor microenvironment (TME) of primary and metastatic colorectal cancer (pCRC and mCRC, respectively). Moreover, we explored if the combination of NK cells with R848, a toll-like receptors 7/8 ligand, could further enhance any pro-inflammatory effects.

Methods Ex vivo expanded umbilical cord blood stem cell derived NK cells were co-cultured with pCRC or mCRC single-cell suspensions in the presence or absence of R848 for 5 days, during and after which flow cytometry and cytokine release profiling were performed.

Results NK cells efficiently induced lysis of tumor cells in both pCRC and mCRC single-cell suspensions and thereby controlled growth rates during culture. They also induced differentiation of infiltrating monocytic cells to an activated DC phenotype. Importantly, this NK-mediated myeloid conversion was also apparent in cultures after tumor cell depletion and was further enhanced by combining NK cells with R848. Moreover, NK cells, and to a greater extent, the combination of NK cells and R848, triggered $CD8^+$ and $CD4^+$ T-cell activation as well as a reduction in activated regulatory T cell rates. Finally, the combination of NK cells and R848 induced a pro-inflammatory shift in the cytokine release profile resulting in higher levels of interferon (IFN)-γ, interleukin (IL)-2, IL-12p70, and IFN-α as well as a reduction in IL-6, in both pCRC and mCRC cultures.

Conclusion Allogeneic NK cells engaged in favorable myeloid crosstalk, displayed effective antitumor activity and, when combined with R848, induced a pro-inflammatory shift of the CRC TME. These findings prompt the investigation of NK cells and R848 as a combination therapy for solid tumors.

WHAT IS ALREADY KNOWN ON THIS TOPIC

⇒ Allogeneic natural killer (NK) cells are gaining interest in the field of cancer immunotherapy because of their ability to directly lyse tumor cells without inducing graft-versus-host disease. Moreover, in mouse models and in in vitro models of human monocyte-derived dendritic cells (DC) NK cells have been shown to activate DC through contact-dependent crosstalk.

WHAT THIS STUDY ADDS

⇒ Here, for the first time, the effects on the human tumor microenvironment of a clinical-stage allogeneic NK cell product were studied in short-term co-cultures with patient-derived single-cell suspensions of primary and metastatic colorectal tumors. We show that these NK cells not only controlled tumor growth but also induced the differentiation of infiltrating monocytic cells to an activated DC-like phenotype. Moreover, alone, but to a greater extent in conjunction with the toll-like receptors 7/8 agonist R848, the NK cells triggered activation of tumor-infiltrating $CD8^+$ and $CD4^+$ T cells, reduced activated regulatory T cell rates, and induced a pro-inflammatory cytokine and chemokine release profile.

HOW THIS STUDY MIGHT AFFECT RESEARCH, PRACTICE OR POLICY

⇒ These findings indicate that allogeneic NK cells may enhance the efficacy of T cell-based immunotherapies and prompt further investigation of their application in the treatment of solid tumors.

INTRODUCTION

Colorectal cancer (CRC) is the third leading cause of cancer worldwide and, despite therapeutic advances, the second cause of cancer-related death.[1] Over the past years, the interest in immunotherapy has risen due

to its success in achieving long-term durable responses in some solid tumors such as melanoma and lung cancer.[2] However, while immune checkpoint inhibitor therapies have been approved for CRC with mismatch repair deficiency or with high levels of microsatellite instability (MSI), clinical outcome in patients who are mismatch repair proficient, microsatellite stable (MSS) or with low levels of MSI, have so far been disappointing, underlining the need for new therapeutic strategies.[2]

Natural killer (NK) cells are innate lymphocytes, mostly known for their ability to lyse virus-infected and cancer cells in absence of prior immune sensitization.[3] Multiple studies have shown that a lower NK cell percentage in blood and lower numbers of infiltrated NK cells in the tumor in patients with CRC correlates with poor overall survival.[4 5] In addition, NK cells derived from patients with CRC often show impaired cytotoxic functionality compared with healthy donors.[6] These findings hint at a role for NK cells in CRC tumor control. Recently, the use of allogeneic NK cells as an anticancer therapy has caught the attention of the scientific community due to the anticancer activity of allogeneic NK cells in the absence of graft-versus-host disease.[7 8] Clinical successes were achieved with allogeneic NK cell therapy for the treatment of acute myeloid leukemia but challenges in the treatment of solid tumors remain, such as migration to the tumor and the immunosuppressive tumor microenvironment (TME).[9] New strategies to overcome these issues are currently being developed, such as genetic modification of NK cells to increase migration efficacy or combination therapies to overcome immunosuppression in the TME.

Besides their direct cytotoxic capacity, NK cells can also affect antitumor immunity through their crosstalk with other immune cells.[3] In particular, NK cells were shown to crosstalk with dendritic cells (DC), that is, professional antigen presenting cells, vital for priming and recruitment of effector T cells, and characterized by high phenotypic plasticity.[10] NK cells have been shown to induce the migration and the maturation of DC, via the production of cytokines (eg, interferon (IFN)-γ and tumor necrosis factor (TNF))[11] and chemokines (eg, X-C Motif Chemokine Ligand (XCL)1 and C-C Motif Chemokine Ligand (CCL)5)[12] as well as via contact-dependent interactions.[11 13 14] Vice versa, DC were found to influence NK cell activity through the release of various cytokines (eg, IFN-α/β, interleukin (IL)-12, IL-18, and IL-15), enhancing their survival, activation and proliferation.[11] Importantly, NK-DC crosstalk can mediate cytotoxic and helper T-cell activation in patients with cancer, leading to increased response to immune checkpoint inhibitors.[15] DC comprise a variety of subsets including conventional DC subsets (cDC1-cDC3), plasmacytoid DC, and inflammatory monocyte-derived DC (MoDC).[16] In the TME, the function of DC can be compromised by various immune suppressive factors, mostly soluble and derived from tumor cells and fibroblasts, including IL-6, IL-10, and prostaglandins, leading to hampered DC differentiation and maturation.[17] The high plasticity of the myeloid lineage complicates the distinction between in particular cDC2, MoDC and monocytes/macrophages and most profoundly so in the TME, where variations in (immune suppressive) cytokine profiles result in a spectrum of macrophage-like and DC-like states that can transition into one another, although in general tumor-promoting M2-like macrophages dominate.[16 18] Thus, besides investigating the direct efficacy of an adoptive NK cell therapy, it is equally important to explore the immune modulatory effects of NK cell therapy in the TME of the host.

In this study we demonstrate that an off-the-shelf allogeneic NK cell therapy, further referred as NK cells, derived from expanded and differentiated umbilical cord blood (UCB) $CD34^+$ hematopoietic stem cells, controls the growth of tumor cells in co-cultures of patient-derived primary or metastatic CRC (pCRC and mCRC, respectively) single-cell suspensions (SCS) as well as induces a shift in monocytic myeloid cells (MoMC) from a macrophage to a DC phenotype and T lymphocyte activation. Moreover, we investigated the combination of NK cells with R848, an agonist for the toll-like receptors (TLR)7/8, which are expressed by various immune cells (including DC, monocytes/macrophages, T cells and NK cells).[19] As TLR7/8 engagement was shown to mediate antitumor responses,[20] we explored whether R848 could induce a more pro-inflammatory TME and thereby support the migration and antitumor activity of NK cells. We show that this combination further enhanced myeloid differentiation and maturation as well as lymphocyte activation. Thus, our data support further exploration of combined allogeneic NK and TLR agonist-based therapies to condition the CRC TME in support of more effective immunotherapy.

METHODS

Hematopoietic stem cell isolation and NK cell culture

The off-the-shelf allogeneic NK cell product (GTA002) (Glycostem Therapeutics, Oss, The Netherlands) was derived from expanded and differentiated $CD34^+$ hematopoietic stem cells. The hematopoietic stem cells were selected from UCB and cultured into fully activated $CD56^+$ NK cells over 28 days and subsequently cryopreserved as previously described.[21] On thawing, the cells were cultured for an additional 5–7 days before use, using the same protocol as before freezing.

Collection and dissociation of primary and metastatic CRC samples

Untreated pCRC and mCRC tissue samples were collected from patients on informed written consent at the Amsterdam UMC (location VU University Medical Center).[22 23] pCRC samples were collected as part of an autologous tumor cell-based vaccination trial from patients with stage I/II CRC.[22] mCRC samples were collected from patients with peritoneal metastasis scheduled for cytoreductive surgery before the start of hyperthermic

intraperitoneal chemotherapy. The samples were enzymatically dissociated into SCS and cryopreserved as previously described.[22 23]

Co-culture of pCRC-SCS and mCRC-SCS and NK cells

pCRC-SCS and mCRC-SCS were co-cultured with NK cells in a 1:1 ratio in the presence or absence of R848 (10 µg/mL, Invivogen). The 1:1 ratio was based on the whole SCS as quantified using a microscope-based counting chamber. 6×10^5 cells from the SCS were plated with and without 6×10^5 NK cells. The cells were incubated at 37°C in a 5% CO_2 humidified atmosphere in a 24 wells plate (Corning) in 600 µL of Roswell Park Memorial Institute medium (RPMI; Gibco) supplemented with 10% fetal calf serum (FCS; Sartorius), 100 U/mL penicillin, 100 µg/mL streptomycin, 0.3 mg/mL glutamine (PSG; Gibco), 0.05 mmol/L 2-mercaptoethanol (2-ME; Merck) and gentamicin/amphotericin (Gibco). After 2 and 5 days, supernatant was collected, cells were harvested with trypsin (Gibco) and subsequentially stained for flow cytometry analysis. Baseline (day 0) staining was also performed. To assess the possible effect of NK cell-mediated tumor control on monocytic differentiation, similar assays

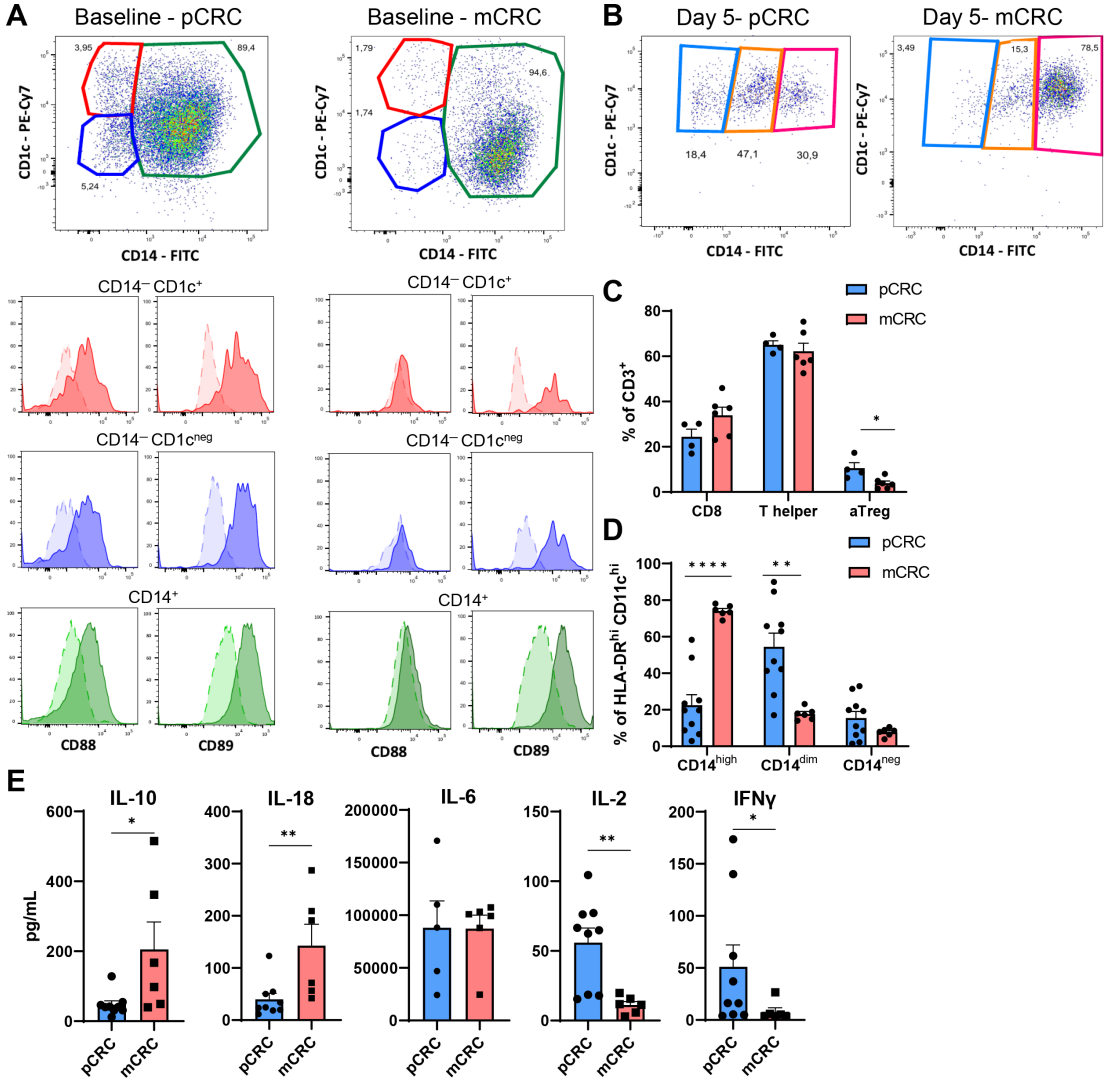

Figure 1 Characterization of the myeloid and lymphocytic compartment of pCRC-SCS and mCRC-SCS. (A) Baseline expression of CD14 and CD1c on myeloid cells defined as CD45$^+$HLA-DR^{hi}CD11c^{hi} and expression of CD88 and CD89 on the different subsets defined by the expression of CD14 and CD1c. Concatenated data; pCRC n=4, mCRC n=6. Darker color: stained; lighter color: FMO. (B) Expression of CD14 and CD1c on myeloid cells defined as CD45$^+$HLA-DR^{hi}CD11c^{hi} after 5 days of culture. Concatenated data; pCRC n=4, mCRC n=6. (C) Differences in the myeloid subsets defined by the expression of CD14 (CD14^{low}, CD14^{dim}, CD14^{hi}) between pCRC (n=9) and mCRC (n=6) after 5 days of culture. (D) Differences in the distribution of CD8$^+$, T helper and aTreg after 5 days of culture. pCRC n=4, mCRC n=6. (E) Cytometry bead array performed on the supernatant of pCRC-SCS or mCRC-SCS after 5 days of culture. pCRC n=9 (IL-6 n=5), mCRC n=6. The data are presented as mean±SEM. Significance is presented as p<0.05*, <0.01**, 0.001***, 0.0001****. P values are determined by two-tailed t-test (C, D) or Mann-Whitney test (E). CRC, colorectal cancer; FITC, fluorescein isothiocyanate, FMO, fluorescence Minus One; IFN, interferon; IL, interleukin; mCRC, metastatic CRC; pCRC, primary CRC; PE-Cy7, PE-Cyanine7; SCS, single-cell suspensions; aTreg, activated regulatory T cells.

were performed by co-culturing tumor cell-depleted pCRC-SCS in the presence or absence of NK cells and/or R848. Due to variable epithelial cell adhesion molecule (EpCAM) expression on tumor cells, the tumor depletion was performed by isolating the $CD45^+$ fraction by magnetic bead-activated cell sorting using CD45 MicroBeads (Miltenyi Biotec) according to the manufacturer's instructions. The mean purity after isolation was 96.3% (SEM: 0.9).

Flow cytometry

Immunophenotypic analyses were performed using flow cytometry (LSRFortessa, BD). A list of all the fluorochrome-conjugated monoclonal antibodies (mAbs) used for cell staining can be found in online supplemental table S1. To perform cell surface staining, the SCS were incubated with mAbs for 20–30 min at 4° in phosphate-buffered saline (PBS, Fresenius Kabi) supplemented with 0.1% bovine serum albumin (Thermo Fisher Scientific) and 0.02% NaN_3 (Merck) (fluorescence-activated cell sorting (FACS) buffer) and subsequently washed with FACS buffer. For intracellular staining (FoxP3 and cytotoxic T-lymphocyte-associated protein 4 (CTLA-4)), the FoxP3 staining kit (eBioscience) was used according to the manufacturer's instructions. Data were analyzed using FlowJo V.10.8.1 (BD Biosciences) or Kaluza V.2.1 (Beckman Coulter).

Cytometric bead array

A cytometric bead array was performed on the supernatants collected from the cultures at day 2 and 5 according to the manufacturer's protocol. A customized LEGENDplex (BioLegend) kit was used containing the following analytes: C-X-C motif ligand (CXCL)9, CXCL10, CXCL11, CCL4, CCL5, CCL20, TNF, IFN-α, IL-10, IFN-γ, IL-12p70, IL-2, IL-15, IL-18. For IL-6 measurements, the human IL-6 Flex Set (BD Bioscience) was used according to the manufacturer's protocol.

Migration assay

Migration assays were performed with the supernatant collected at day 2 from the cultures of pCRC-SCS and mCRC-SCS with and without R848. NK cells were thawed 7 days prior to the assay. At the time of the migration assay, the NK cells were washed with PBS (Lonza) and resuspended in unconditioned medium (RPMI supplemented with 10% FCS, PSG, 2-ME, and gentamicin/amphotericin). Supernatants were added to the lower compartment of a 96-transwell plate with 5 µm pore filter size (Corning). As a control, unconditioned medium was added in the lower compartment to measure spontaneous migration. Subsequently, 5×10^5 NK cells were loaded into the transwell and allowed to migrate for 3.5 hours. After incubation, migrated cells were counted in the lower compartment. Percentage of migration was calculated as follows: % migration=(number of migrated $CD56^+$ cells – number of spontaneous migrated $CD56^+$ cells)/(number of total $CD56^+$ cells – number of spontaneous migrated $CD56^+$ cells)×100%.

Cytotoxicity assay

To explore the cytotoxic potential of NK cells, cytotoxicity assays were performed using pCRC-SCS and mCRC-SCS. The cells were co-cultured in an NK:SCS ratio of 1:1 in a total volume of 200 µL RPMI in a 96 wells plate (Sarstedt). The readout was based on absolute numbers of alive tumor cells [$Epcam^+CD45^-$7-aminoactinomycin D $(7AAD)^-$] quantified with Quantibrite Beads (Invitrogen, Thermo Fisher Scientific) and it was performed after 1, 2, 5 and/or 7 days.

Statistical analysis

Statistical analysis was performed using GraphPad Prism software. Normality was assessed using the Shapiro-Wilk test and the statistical tests were selected accordingly. To analyze the differences between pCRC and mCRC at baseline and at day 5, two-tailed t-test or the Mann-Whitney U test were used. One-way analysis of variance (ANOVA) with Tukey multiple comparison analysis or Friedman test with Dunn's multiple comparison analysis were used to assess the effects in co-cultures of NK cells and/or R848 on the pCRC-SCS or mCRC-SCS and vice versa. Means (and SEM) of obtained data and which statistical tests were used can be found in online supplemental tables S1–S5. Two-way ANOVA with Tukey multiple comparison analysis was used to compare the effects of NK cells and/or R848 on the tumor cell-depleted and non-depleted pCRC-SCS. Finally, a correlation analysis was performed using R V.4.0.3. The correlation coefficients were calculated using the Spearman rank-order correlation analysis. Significance is presented as p<0.05*, <0.01**, 0.001***, 0.0001****.

RESULTS

Characterization of the myeloid and lymphocytic compartments of pCRC-SCS and mCRC-SCS

We first set out to identify and characterize the myeloid DCs in cryopreserved SCS from untreated pCRC and mCRC lesions. To this end, we gated $CD45^+$ cells expressing high levels of HLA-DR and CD11c. To avoid contamination of B cells (that share markers with DCs), lymphocytes were excluded from our gating strategy based on scatter properties. The employed gating strategy is shown in online supplemental figure S1. At baseline, we identified three main $CD45^+$HLA-$DR^{hi}CD11c^{hi}$ populations based on the differential expression of CD1c and CD14: $CD14^-CD1c^+$, $CD14^-CD1c^-$, and $CD14^+$, the latter of which was clearly the predominant population in both pCRC and mCRC samples (figure 1A) with a slightly higher, although statistically significant, presence in mCRC samples (online supplemental figure S2A). All three subsets in pCRC were found to express both CD88 and CD89, both previously shown to be restricted to cells of monocytic origins[18 24] while the subsets in mCRC mainly expressed CD89 (figure 1A), showing that all $CD45^+$HLA-$DR^{hi}CD11c^{hi}$ cells detectable in both pCRC and mCRC

were MoMC, most likely representing a differentiation continuum from monocytes/macrophages ($CD1c^-$ $CD14^+$) to MoDCs ($CD1c^+CD14^-$). Predominance of the $CD14^+$ subset is consistent with an immune suppressed milieu unsupportive of DC differentiation.[25] We did not detect any bona fide $CD88/89^-$ CD141/BDCA3$^+$ cDC1 or $CD1c^+$ cDC2, also not when gating included the lymphocyte population and $CD11c^{dim}$ cells, which might have comprised cDC1 (data not shown). Of note, no baseline differences in the percentages of $CD45^+$ and $CD45^-$ cells were found between pCRC and mCRC samples (online supplemental figure S2B).

After 5 days of culture, all $CD45^+$HLA-$DR^{hi}CD11c^{hi}$ cells expressed CD1c, indicative of a shift to a more DC-like phenotype.[25] Post-culture, three subpopulations could be defined based on the expression of CD14:$CD14^{neg}$, $CD14^{dim}$, and $CD14^{hi}$ (figure 1B) with the latter most likely representing a more suppressed, M2-macrophage-like phenotype.[25] All three MoMC populations maintained expression of CD88 and CD89 with some variation in intensity (online supplemental figure S3). Interestingly, these populations were not equally distributed in pCRC and mCRC, as mCRC-SCS showed a higher percentage of $CD14^{hi}$ cells, while higher levels of $CD14^{dim}$ cells were found in pCRC-SCS (figure 1B,C). This difference most likely indicates a higher level of immune suppression in metastatic lesions.

At baseline and at day 5, lymphocyte content was also assessed and the distribution of $CD8^+/CD4^+$ T cells was analyzed. For the employed lymphocyte gating strategy, see online supplemental figure S4. pCRC-SCS comprised higher levels of activated regulatory T cells (aTreg; defined as $FoxP3^+CD45RA^-CD25^{high}$)[26] compared with mCRC-SCS both as baseline and after 5 days of culture, whereas no significant difference was found in $CD8^+$ and T helper (Th) cell rates (figure 1D, online supplemental figure S2C). Analysis of supernatants after 5 days of culture revealed that mCRC released higher levels of the pleiotropic cytokines IL-10 and IL-18[27 28] whereas the levels of IL-2 and IFN-γ, two cytokines produced by activated NK and T cells,[29 30] were lower, again consistent with a state of more profound immune suppression (figure 1E).

Maintained activated phenotype and tumor cytolytic functionality of NK cells in the CRC TME

We assessed the migration capacity of NK cells towards the supernatant of 2-day pCRC samples. After 3.5 hours of NK cell seeding, 24.2% of the NK cells had actively migrated towards the supernatant of the pCRC samples. This was only marginally, though significantly, increased to 27.0% when R848 was added to the tumor culture (figure 2A). Despite the expected higher immune suppressive state of the mCRC samples, similar levels of active NK cell migration were observed towards the supernatant of the mCRC samples. In this setting, no R848-related benefit was observed (figure 2A). This data indicates that the TME of both pCRC and mCRC express chemokines that can actively attract NK cells.

Next, the stability of the NK cell phenotype on co-culture with pCRC and mCRC samples was assessed. Expression levels of different activating and inhibitory receptors known to affect NK cell activity were measured on NK cells at baseline and after 5 days of co-culture with either pCRC or mCRC, or without either as control. Baseline expression levels were consistent with an activated profile as previously described,[31] with particularly high expression of the activating receptors NKG2D, DNAM-1, NKp44 and NKp46, and low expression of the inhibitory receptor KIR2D (figure 2B,C, online supplemental tables S2 and S3). Of note, the analysis of the corresponding ligands revealed their expression on both pCRC-derived and mCRC-derived tumor cells (online supplemental figure S5), indicating that these could potentially initiate activation of NK cells. Interestingly, the NK cell phenotype remained mostly unaffected after 5 days of co-culture with either pCRC or mCRC samples, in the absence or presence of R848, suggesting that pCRC or mCRC samples did not negatively affect the cytolytic potential of NK cells (figure 2B,C). Differences were observed for NKG2C and CD25, which was probably due to cytokine withdrawal as this effect was also observed in the medium only condition (without tumor added) (figure 2B,C). In addition, no significant direct effect of R848 was observed on NK cells after 5 days of co-culture, except for a small decrease in NKp30 expression (online supplemental figure S6A). We also determined expression levels of TLRs by whole transcriptome RNA sequencing and observed no expression of TLR7 and very low levels of TLR8 in the allogeneic NK cells (online supplemental figure S6B), supporting our finding that R848 did not directly impact the NK cells.

Finally, the cytolytic capacity of NK cells was assessed in a 5-day assay by co-culturing NK cells with pCRC or mCRC samples in the presence or absence of R848 (figure 2D). While after 1 day no significant decrease in absolute numbers of $EpCAM^+CD45^-7AAD^-$ tumor cells was found, at day 5, a significant reduction of the numbers of tumor cells was observed in both pCRC and mCRC samples proving that NK cells were able to efficiently control tumor growth. No added benefit from the addition of R848 was observed in this respect. More refined kinetic analysis of tumor growth control in pCRC-SCS cultures (with variable tumor HLA class-I expression levels, online supplemental figure S7A) revealed a loss of absolute numbers of live tumor cells (defined as $EpCAM^+CD45^-7AAD^-$) in all conditions from day 1 to day 2 and a steady subsequent increase over time up to day 7, which was only marginally controlled by R848, but profoundly inhibited in the presence of NK cells (online supplemental figure S7B). To assess the possible contribution to the observed tumor growth control of $CD8^+$ cytotoxic T cells, all cultures were also conducted in the presence of HLA-ABC-blocking antibodies. No differences were found in any of the conditions (online supplemental figure S7B), suggesting that $CD8^+$ T cells did not contribute to tumor lysis.

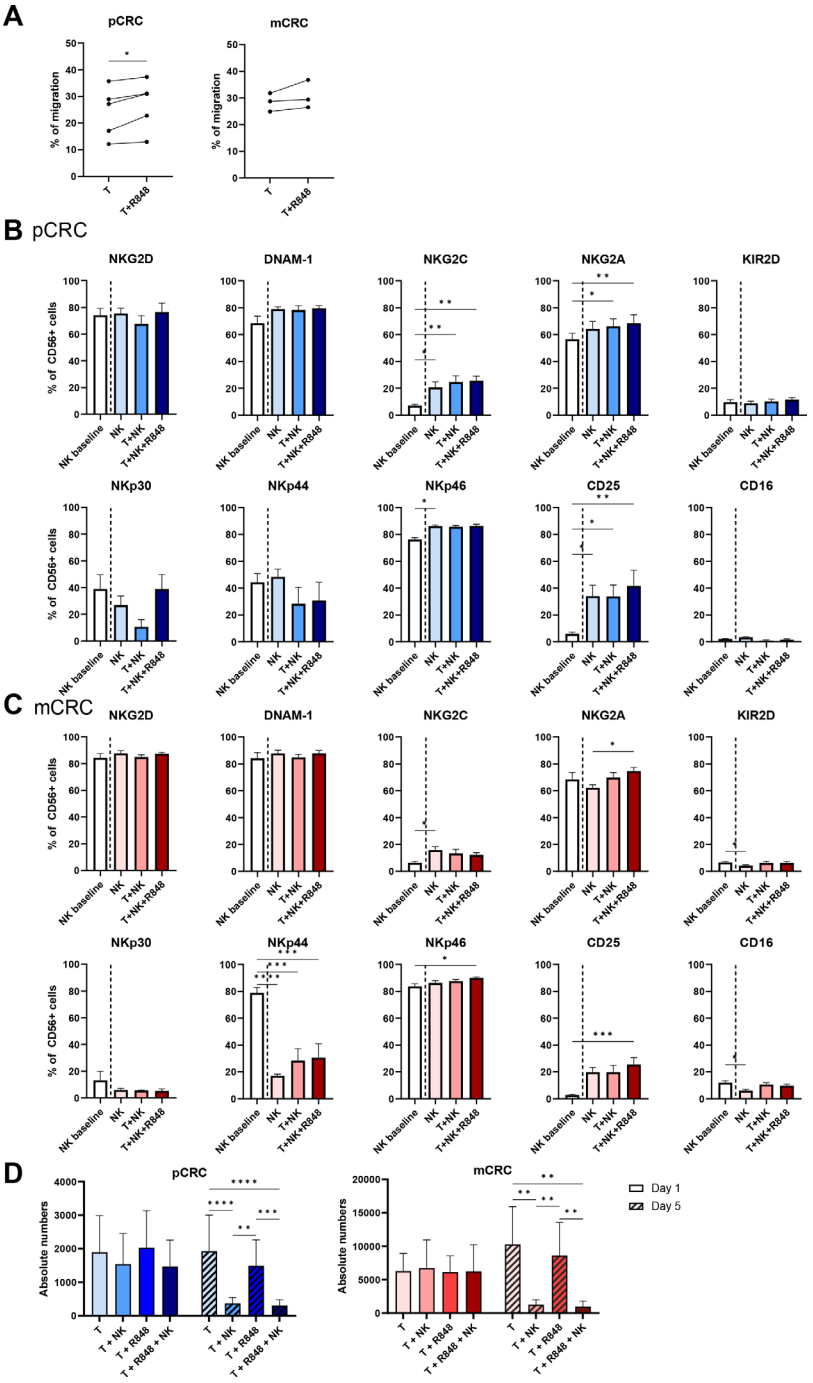

Figure 2 NK cell phenotype on 5-day co-culture with pCRC-SCS or mCRC-SCS in the presence and absence of R848. (A) Specific migration of NK cells towards supernatant of the conditions T and T+R848 at day 2 (pCRC: n=5; 2 NK donors, mCRC: n=3; 2 NK donors). Spontaneous migration averaged 22.7% (SEM=0.92) of total NK cells which was subtracted from the specific migration. (B,C) Receptor expression (in percentage) at day 5 of NK cells in co-culture with (B) pCRC-SCS (n=5; 3 NK donors) or (C) mCRC-SCS (n=6; 3 NK donors). As a control, medium only was taken along. NK cell:SCS ratio of 1:1 (D) Absolute number of Epcam^{+}CD45^{-} tumor cells of pCRC-SCS (n=7; 2 NK donors) and mCRC-SCS (n=4; 2 NK donors) ± NK cells ± R848 for 1 and 5 days at an NK cell:SCS ratio of 1:1. The data are presented as mean±SEM. Significance is presented as p<0.05*, <0.01**, 0.001***, 0.0001****. P values were determined by two-tailed paired t-test analysis (A) one-way ANOVA with Tukey multiple comparison analysis, Friedman test with Dunn's multiple comparison analysis (B,C) or two-way ANOVA with Tukey multiple comparisons analysis (D). ANOVA, analysis of variance; CRC, colorectal cancer; EpCAM: epithelial cell adhesion molecule, mCRC, metastatic CRC, NK, natural killer; pCRC, primary CRC; SCS, single-cell suspensions; T, tumor.

NK cell-induced DC conversion of MoMC in pCRC and mCRC cultures

We next explored the effect of NK cells, both in the presence and absence of R848, on the myeloid compartment. pCRC-SCS and mCRC-SCS were co-cultured with NK cells and/or R848 (figure 3; online

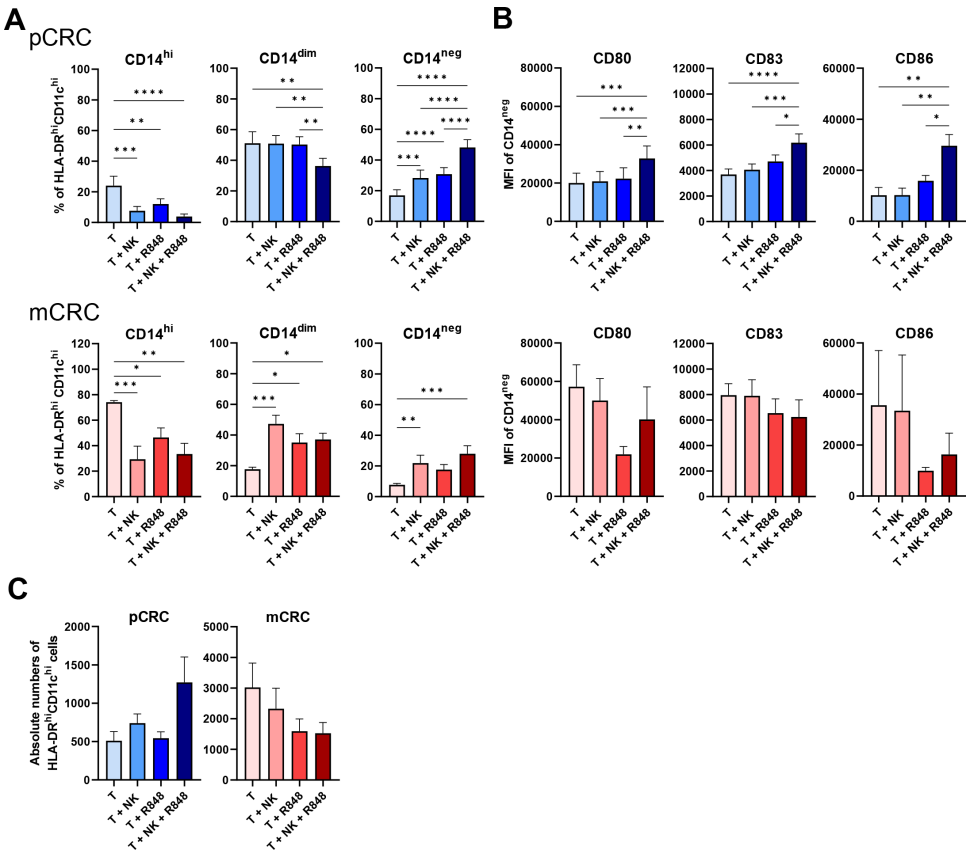

Figure 3 NK cells induce CD14 downregulation on pCRC and mCRC myeloid cells and, when combined with R848, maturation of CD14^{neg} pCRC myeloid cells after a 5 day co-culture with pCRC-SCS or mCRC-SCS. (A) Changes in the percentages of CD14^{hi}, CD14^{dim}, CD14^{neg} and (B) in the expression level (in mean fluorescence intensity (MFI)) of CD80, CD83 and CD86 on CD14^{neg} cells. pCRC: n=9; 3 NK donors, mCRC: n=6; 3 NK donors. (C) Absolute numbers of myeloid cells (defined as CD45^{+}HLA-DR^{hi}CD11c^{hi}). NK cell:SCS ratio: 1:1 (A, B, C). The data are presented as mean±SEM. Significance is presented as p<0.05*, <0.01**, 0.001***, 0.0001****. P values are determined by one-way analysis of variance with Tukey multiple comparison analysis or Friedman test with Dunn's multiple comparison analysis (mCRC: MFI of CD80, CD83 and CD86) (A, B). CRC, colorectal cancer; mCRC, metastatic CRC; NK, natural killer; pCRC, primary CRC; SCS, single-cell suspensions; T, tumor.

supplemental tables S4 and S5). In both pCRC and mCRC, the presence of NK cells induced CD14 downregulation on MoMC leading to a shift towards a CD14^{neg} phenotype. Interestingly, this shift was more pronounced in pCRC where higher rates of CD14^{neg} MoMC were reached whereas in mCRC the conversion was incomplete leading to increased levels of CD14^{dim} MoMC (figure 3A). In pCRC, the addition of R848 further reinforced the NK cell effect and induced a more complete shift towards a DC-like state, supported by simultaneous upregulation of CD80, CD86 and CD83 on CD14^{neg} MoMC consistent with a mature cDC phenotype (figure 3B). Of note, R848 was selected for combination therapy with the NK cells after a preliminary analysis conducted on cultures from five pCRC samples, evaluating the effect of combining NK cells with either R848, poly I:C (TLR3-ligand) or stimulator of interferon genes (STING) ligands (cyclic-di-AMP and rr-cyclic-di-AMP). These analyses showed R848 to be superior in supporting the stimulatory effect of the allogeneic NK cells on both monocyte-to-DC conversion and CD80 and CD83 upregulation on CD14^{neg} MoMC (online supplemental figure S8). The presence of R848 in mCRC did not enhance the NK cell mediated CD14 downregulation. Moreover, no upregulation of co-stimulatory maturation markers on CD14^{neg} MoDC was observed. Effects on the expression of T-cell immunoglobulin mucin 3 (Tim3), Programmed Cell Death Ligand 1 (PD-L1), and human blood dendritic cell antigen 3 (BDCA3)/CD141 on MoMC were also assessed and can be found in online supplemental tables S4 and S5. Finally, as NK cells were reported to selectively lyse immature DC,[32] we assessed if these changes in subset distribution were accompanied by a decrease in the absolute number of CD45^{+}HLA-DR^{hi}CD11c^{hi} cells. No significant reductions in the absolute number of myeloid cells were found in either pCRC- or mCRC-SCS, in the presence of both NK cells and R848 (figure 3C). Rather, a trend of increased CD45^{+}HLA-DR^{hi}CD11c^{hi} cell numbers was observed in the pCRC samples, suggestive of their increased survival during culture.

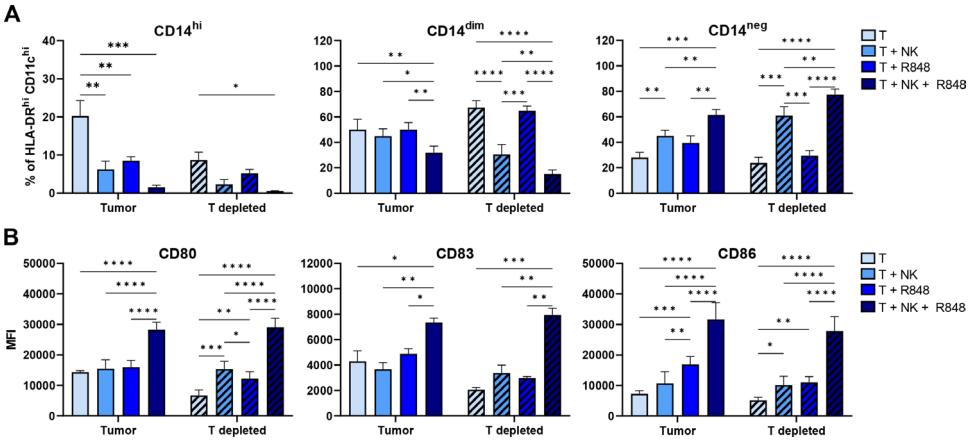

Figure 4 The effect of NK cells, alone or in combination with R848, on pCRC myeloid cells is not due to their ability to control tumor growth. The graphs show changes (A) in the percentages of $CD14^{hi}$, $CD14^{dim}$, $CD14^{neg}$ and (B) in the expression of CD80, CD83 and CD86 on $CD14^{neg}$ cells after 5 days of culture. The myeloid cells were defined as $CD45^{+}HLA\text{-}DR^{hi}CD11c^{hi}$. n=3; 2 NK donors. NK cell:SCS ratio 1:1. The data are presented as mean±SEM. Significance is presented as p<0.05*, <0.01 **, 0.001***, 0.0001****. P values are determined by two-way analysis of variance with Tukey multiple comparison analysis. NK, natural killer; pCRC, primary colorectal cancer, SCS, single-cell suspensions; T, tumor.

NK cell-induced DC conversion among CRC-derived MoMC is not due to tumor cell deletion

As we demonstrated that NK cells simultaneously induced DC conversion and tumor lysis in CRC cultures, the question arose whether this effect of NK cells on the MoMC compartment could be wholly attributed to the decrease in tumor load and the associated immune suppression in the cultures. After 5 days, when tumor cells were depleted from pCRC-SCS (by positive $CD45^{+}$ cell selection), NK cells still induced downregulation of CD14 on MoMC, suggesting that the observed DC-like differentiation was truly due to NK-MoDC crosstalk and not affected by mere elimination of immune suppressive tumor cells (figure 4A). Unmodulated tumor-depleted cultures did show a relative shift from a $CD14^{hi}$ to a $CD14^{dim}$ state (online supplemental figure S9), confirming that the $CD14^{+}$ macrophage-like state was tumor-induced. Interestingly, while the combination of NK cells and R848 did increase the percentage of $CD14^{neg}$ MoMC, no differences were found in the presence of only R848 compared with the depleted tumor control (figure 4A). This indicates that, whereas in the presence of tumor cells, R848 substantially contributes to the conversion to a $CD1c^{+}CD14^{neg}$ DC-like state, in the absence of tumor cells, this process is less dependent on the presence of R848 and dictated solely by NK/DC crosstalk. The expression of the DC maturation and co-stimulatory molecules CD80, CD83, and CD86 on $CD14^{neg}$ MoMC was also analyzed (figure 4B); maturation induction required the combination of both NK cells and R848, irrespective of the presence of tumor cells.

Higher level T-cell activation and a reduction in aTreg rates in both pCRC and mCRC induced by NK cells in combination with R848

As NK-DC crosstalk has been described to induce cytotoxic T-cell activation,[11] we also tested this in our model (figure 5; online supplemental tables S4 and S5). In pCRC, the addition of NK cells induced higher levels of CD25 expression on both $CD8^{+}$ T cells and Th cells whereas in mCRC this was only observed in the presence of both NK cells and R848 (figure 5A,B). Moreover, in pCRC, higher rates of $CD8^{+}CD69^{+}$ cells were found in the presence of both NK cells and R848. These results show that NK cells can induce T-cell activation in pCRC which is further enhanced by the addition of R848. In contrast, in mCRC, significant effects were only observed when NK cells were combined with R848. Interestingly, in pCRC, the combination of NK cells and R848 induced an increase in $Tim3^{+}CD8^{+}$ T cells while no effects on the expression of other immune checkpoint receptors were observed (online supplemental figure S10; online supplemental tables S4 and S5). In addition, in mCRC but not in pCRC NK cells induced CTLA-4 downregulation on Th cells (online supplemental figure S10).

In the presence of NK cells, we observed a decrease in the percentage of aTregs in both pCRC and mCRC samples as well as a decrease in absolute numbers of aTregs in pCRC, whereas in mCRC cultures, the absolute number of aTregs was significantly reduced only in the presence of both NK cells and R848 (figure 5C,D). No changes in absolute numbers of $CD8^{+}$ T cells and Th cells were observed leading to a significant increase in the CD8/aTreg ratio in both pCRC and mCRC-SCS, when NK cells and R848 were combined, consistent with a more T-cell inflamed TME (figure 5E). We assessed if NK cells were able to directly lyse aTregs in the pCRC cultures (defined as $FoxP3^{+}CD45RA^{-}CD25^{high}$), as previously reported.[33] To this end, we performed a 24 hours cytotoxicity assay by co-culturing aTreg enriched pCRC samples (mean % aTreg=12.44±4.83) with NK cells (online supplemental figure S11A). As no significant decrease in the absolute number of live aTregs was observed, we concluded that

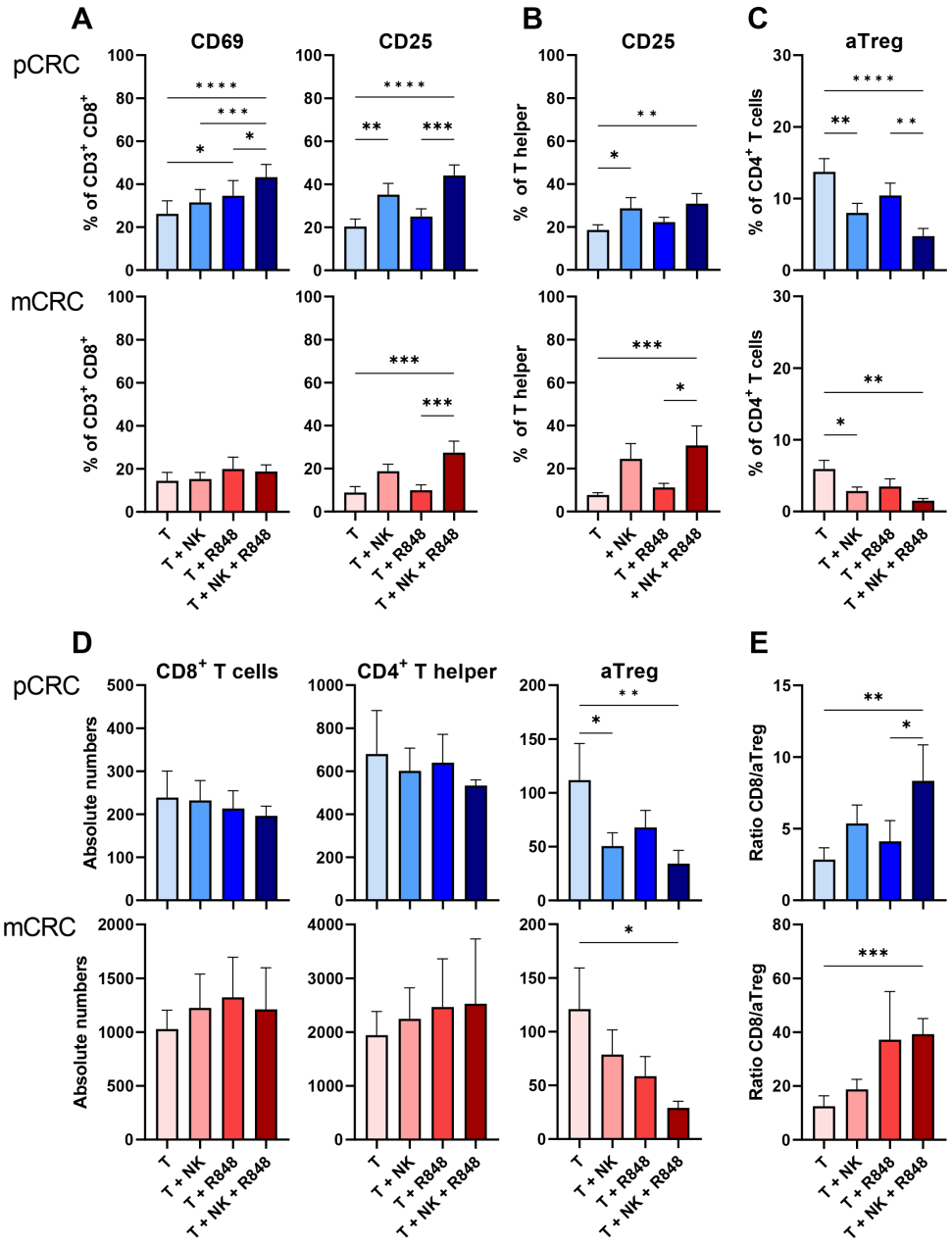

Figure 5 NK cells in combination with R848 induce CD8$^+$ T cell and T helper activation and decrease activated Treg (aTreg) rates. (A) Percentages of CD69$^+$ and CD25$^+$ CD8$^+$ T cells. (B) Percentage of CD25$^+$ CD4$^+$ T helper cells. (C) Percentage of aTreg in CD4$^+$ T cells. (D) Absolute number of CD8$^+$ T cells, CD4$^+$ T helper or aTreg. (E) CD8/aTreg ratio calculated based on the absolute number of CD8$^+$ T cells and aTreg. pCRC: n=9; 3 NK donors (A–C) and pCRC: n=4; 2 NK donors (D, E) mCRC: n=7; 3 NK donors (A–C) and mCRC: n=6, 3 NK donors (D, E). NK cell:single-cell suspensions ratio 1:1 (A–E). Readouts performed after 5 days of culture. The data are presented as mean±SEM. Significance is presented as p<0.05*, <0.01**, 0.001***, 0.0001****. P values are determined by one-way analysis of variance with Tukey multiple comparison analysis or Friedman test with Dunn's multiple comparison analysis ((B) mCRC (D) mCRC T helper). CRC, colorectal cancer; mCRC, metastatic CRC; NK, natural killer; pCRC, primary CRC; T, tumor; Treg, regulatory T cells.

NK cells did not directly induce aTreg death (online supplemental figure S11B). Finally, considering the key role of transforming growth factor (TGF)-β in aTreg development and functionality,[34] we assessed whether the observed aTreg reduction was related to decreased levels of this cytokine. No differences in the levels of TGF-β were found, suggesting that other factors were involved in the observed reduction in aTreg rates (online supplemental figure S11C).

NK cell-induced changes in the pCRC and mCRC cytokine and chemokine release profiles

To better understand the effect of NK cells alone or in combination with R848 on the inflammatory state of the TME, cytokine and chemokine profiling was performed using supernatants of the 5-day pCRC or mCRC cultures (figure 6). Of note, similar cytokine and chemokine profiles were found in day 2 supernatants (online supplemental figure S12). The combination of NK cells

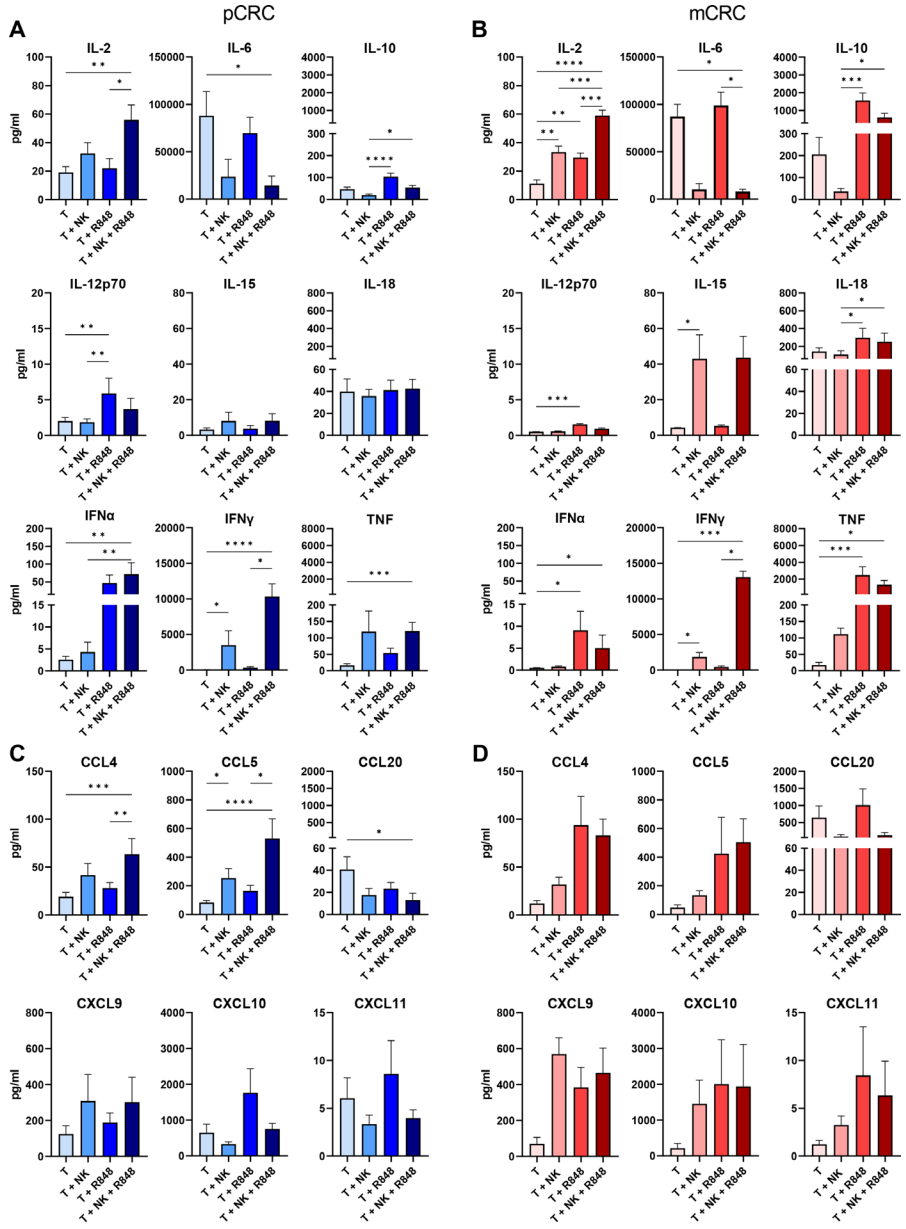

Figure 6 Changes in the cytokine and chemokine profile on co-culture of pCRC-SCS or mCRC-SCS with or without NK cells and/or R848. Cytometry bead array performed on the supernatant of pCRC-SCS or mCRC-SCS cultured for 5 days in the presence and absence of NK cells and/or R848. NK cell:SCS ratio 1:1. Cytokine levels: (A) pCRC-SCS and (B) mCRC-SCS. Chemokine levels: (C) pCRC-SCS and (D) mCRC-SCS. pCRC: n=9; 3 NK donors (IL-6 n=5), mCRC: n=6: 3 NK donors. The data are presented as mean±SEM. Significance is presented as p<0.05*, <0.01**, 0.001***, 0.0001****. P values are determined by Friedman ANOVA with Dunn's multiple comparison analysis or one-way ANOVA with Tukey multiple comparison analysis (pCRC and mCRC: IL-2, CCL4). ANOVA, analysis of variance; CCL, C-C Motif Chemokine Ligand; CRC, colorectal cancer; CXCL, X-C Motif Chemokine Ligand; IFN, interferon; IL, interleukin; mCRC, metastatic CRC, NK, natural killer; pCRC, primary CRC; SCS, single-cell suspensions; T, tumor.

and R848 resulted in a decrease of the pro-tumorigenic cytokine IL-6[35] and an increase of IFN-γ, TNF, and IL-2 levels in pCRC samples. Independently of the presence of NK cells, R848 induced higher release of IL-12p70, IFN-α, and IL-10, most likely due to the stimulation of myeloid cells (figure 6A).[36] The analysis of the supernatants of mCRC-SCS showed a similar trend for IL-6, IFN-γ, and IL-2 (figure 6B). However, R848 induced a dramatic increase in IL-10 and TNF specifically in mCRC. Moreover, while R848 still induced increases in IL-12p70 and IFN-α, the levels of these cytokines were lower compared with the pCRC samples, which may be related to the differences in myeloid composition between pCRC and mCRC samples. Finally, in mCRC samples, higher levels of IL-15 were observed in the presence of NK cells (figure 6B). CCL4 and CCL5, both able to attract DCs to the TME,[12 37] were secreted by the pCRC samples, and concentrations were increased on NK cell addition (figure 6C). In mCRC samples, the increase of CCL4 and

CCL5 concentrations seemed to be more R848 dependent (figure 6D). The chemokines CXCL9, CXCL10, and CXCL11 are ligands for the CXCR3 receptor, which is expressed on activated effector T and NK cells and higher levels of these chemokines are known to correlate with better survival in patients with CRC.[38] We found detectable levels of the effector T and NK cell-attracting chemokines CXCL9 and CXCL10 (both previously correlated to

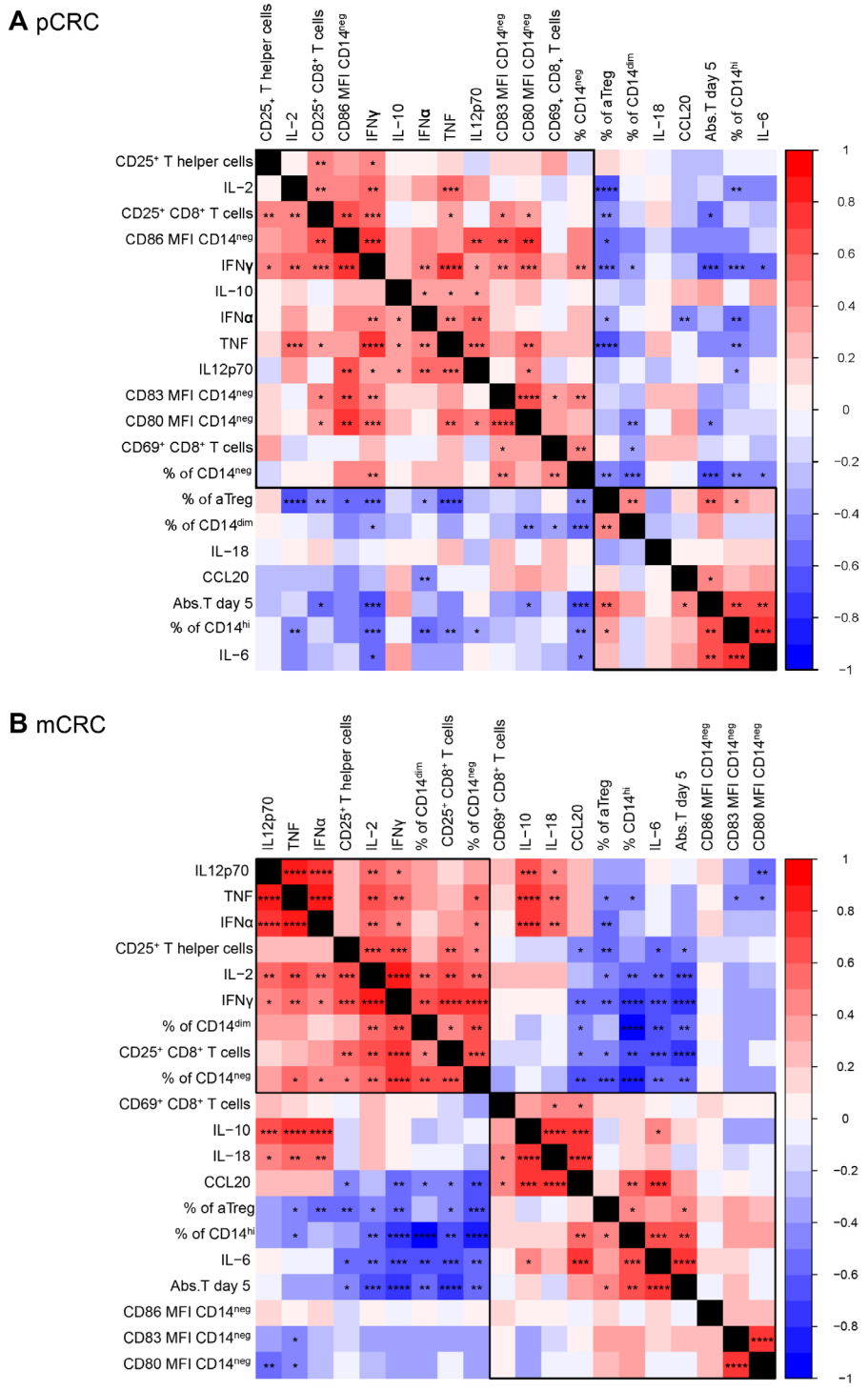

Figure 7 Correlation analysis reveals a dichotomy between pro-inflammatory and immune suppressive factors related to monocytic dendritic cell activation in both pCRC and mCRC models. Correlation plot based on (A) pCRC-SCS and (B) mCRC-SCS. The analysis has been performed including data from all the analyzed conditions (eg, tumor only, tumor with R848 and/or NK cells). pCRC: n=9; 3 NK donors, mCRC: n=7; 3 NK donors. Correlation coefficient and p values are determined by Spearman correlation analysis. Significance is presented as p<0.05*, <0.01**, 0.001***, 0.0001****. Abs, T day 5, absolute number of tumor cells at day 5; CRC, colorectal cancer; IFN, interferon; IL, interleukin; mCRC, metastatic CRC; MFI, mean fluorescence intensity; NK, natural killer; pCRC, primary CRC; SCS, single-cell suspensions; TNF, tumor necrosis factor.

improved survival in CRC)[38] in the tumor-only condition, which were increased by NK cells, R848, or the combination of both, with more pronounced differences in the mCRC samples, probably as a result of the increased TNF and IFN-γ concentrations (figure 6C,D).[39] Finally, levels of the chemokine CCL20, known to contribute to tumor progression by attracting Tregs to the TME,[40] were much higher in the mCRC samples (figure 6C,D). When NK cells were added, the concentration was decreased, suggesting a shift towards a less immune suppressive TME (figure 6D).

Correlation analysis revealed a dichotomy between pro-inflammatory and immune suppressive factors in both pCRC and mCRC models

A correlation matrix analysis was performed separately on the data collected from the pCRC (figure 7A) and mCRC (figure 7B) cultures, comprising all tested conditions (ie, medium control, NK cells, R848, NK cells+R848). In both pCRC and mCRC single-cell cultures, two main groups of correlating parameters were found, based on the hierarchical clustering order, revealing concerted regulation of pro-inflammatory versus immune suppressive pathways. One group comprised the percentage of $CD14^{hi}$ macrophage-like MoMC, the percentage of aTregs, the absolute number of tumor cells and the levels of IL-6 (ie, concerted immune suppression). The other group comprised markers of T-cell activation, Th1 cytokines (IFN-γ, IL-2, TNF), the percentage of $CD14^{neg}$ DC-like MoMC and, in pCRC samples, the expression of DC maturation markers (CD80, CD83, CD86) on $CD14^{neg}$ DC-like MoMC (ie, concerted immune activation) (figure 7B).

DISCUSSION

Interest in off-the-shelf allogeneic NK cell therapies is increasing now that allogeneic NK cells have proven to be safe and show efficacy in hematological malignancies and, to a lesser extent, in solid tumors.[41] As NK cells can also influence the activity of other immune cells, exploring the potential effects of allogeneic NK cell products on the TME is important to better understand their full mode of action. Here, we report that the allogeneic UCB $CD34^{+}$ stem cell-derived NK cell therapy induced changes in the TME as modeled in short-term co-cultures of NK cells and pCRC-SCS or mCRC-SCS, either alone or in combination with R848, a TLR7/8 ligand. We observed that NK cells, especially when combined with R848, induced downregulation of CD14 on MoMC and simultaneous upregulation of DC-related maturation/co-stimulatory markers, depletion of aTregs, activation of $CD8^{+}$ and Th cells, and the production of various pro-inflammatory cytokines and chemokines. NK cell products may thus present a promising new immunotherapy for solid tumors like CRC. In particular, in peritoneal CRC metastases which were shown to be predominantly CMS4 CRC tumors, characterized by high Treg and TGF-β levels and related to poor prognosis and response to systemic therapies,[42 43] we observed that NK cells still provided potent growth control of tumor cells and that the combination of NK cells and R848 was able to induce a pro-inflammatory shift in the TME, despite its more immunosuppressive status than that of pCRC. In addition, as NK-DC crosstalk was shown to be involved in anti-programmed cell death protein 1 (PD-1) mAb induced antitumor responses,[15] combined NK cell/R848 therapy may facilitate successful immune checkpoint blockade in relatively resistant tumors like MSS-CRC.[2]

In the pCRC-SCS and mCRC-SCS used in this study, we found three main subsets of $CD88/CD89^{+}$ MoMC,[18 24] based on different CD1c and CD14 expression. Based on our previous work,[44 45] the expression of CD14 on MoMC defines different functional states with $CD14^{neg}$ MoMC representing a more DC-like and $CD14^{hi}$ MoMC a more suppressive/M2-macrophage-like subset.[44 45] In line with this, in both pCRC and mCRC single-cell cultures, we observed that the percentage of $CD14^{hi}$ MoMC inversely correlated with the concentration of the Th1 cytokines IFN-γ, TNF, and IL-2,[29 30] whereas it was positively associated with various suppressive factors (ie, the percentage of aTreg, the concentration of IL-6 and the absolute number of tumor cells). In contrast, the percentage of $CD14^{neg}$ DC-like MoMC positively correlated with the activation status of T cells and the release of Th1 cytokines. These differential associations are thus consistent with the proposed functional states of these $CD14^{+}$ subsets.

Differential immune modulatory effects of NK cells with or without R848 were observed between pCRC-SCS and mCRC-SCS cultures. Whereas maturation of $CD14^{neg}$ MoMC and T-cell activation was observed on NK cell addition in pCRC samples, DC-maturation was not observed in mCRC samples and T-cell activation was limited. Strikingly, the levels of $CD14^{neg}$ MoMC activation in mCRC were already high in the tumor only culture, which might have been related to high levels of IL-6 and/or CRC-associated prostaglandins, which we previously showed to contribute to MoDC activation.[46] In addition, higher levels of the anti-inflammatory IL-10, lower levels of the pro-inflammatory IL-2 and IFN-γ, and higher levels of $CD14^{hi}$ MoMC were detected in mCRC samples, suggesting a more immune suppressive TME. Higher levels of IL-18 release were also found in mCRC. IL-18 is a pleiotropic cytokine involved in the activation and differentiation of various lymphocytes[28] IL-18 was shown to have pro-metastatic potential in mice[47] and, similarly to IL-10, its expression levels in patients with CRC correlated with advanced tumor stages, larger tumor size, poor tumor cell differentiation, and the presence of distant metastases.[40]

The observed differences in the TME of pCRC versus mCRC also became apparent in a differential response to R848. In mCRC, R848 mediated a strong increase in the levels of IL-10, IL-18, and TNF accompanied by a small increase in IL-12p70 and IFN-α. In contrast, in pCRC, R848 stimulation induced higher levels of IFN-α and IL-12p70 whereas just a small increase in IL-10 was observed with no changes in IL-18 release. As all these

cytokines can be produced by activated macrophages and by DC,[36 47–49] these observed differences might be due to the divergent composition of the myeloid compartment. Based on these findings, it is likely that the administration of NK cells and R848 to patients with more advanced CRC, might benefit from the combination with, for example, an STAT3 inhibitor that was previously shown to counteract the detrimental effect of IL-10 on MoDC differentiation.[44] It is noteworthy that despite the more suppressive TME of mCRC samples, the cytotoxic capacity of the NK cells was not affected in mCRC-SCS and no significant differences were found in the expression of key functional NK cell receptors such as NKG2D and DNAM-1, suggesting that, while a more suppressive environment can limit the pro-inflammatory effect of NK cells on the TME, it does not hamper its cytotoxic capacity.

We observed that the NK cells induced T-cell activation, and to a larger extent when combined with R848, as shown by the higher levels of CD25 and CD69 as well as by the increased concentration of IFN-γ, TNF, and IL-2 in co-cultures of NK cells and CRC-SCS. Still, $CD8^+$ T cells did not seem to contribute to the tumor growth control observed in the presence of NK cells. However, the high NK cell-to-tumor ratio in our cultures might have limited any $CD8^+$ T cell effect and under different circumstances (eg, in vivo) this activation might translate into a more synergistic or additive antitumor effect. Besides $CD8^+$ T-cell activation, NK cells, alone or in combination with R848, induced a profound reduction in the percentage of aTregs. Although it has been reported that NK cells from peripheral blood can directly lyse aTregs,[33] no direct cytotoxicity was found after a 24 hours co-culture with aTreg enriched pCRC samples and stem cell-derived NK cells. It has also been described that NK cells can prevent the CD28-mediated FoxP3 expression on naïve $CD4^+CD25^-$ T cells via the release of IFN-γ.[50] In both pCRC-SCS and mCRC-SCS cultures, the percentage of aTregs inversely correlated with IFN-γ, while it correlated with the absolute number of tumor cells and the levels of IL-6.[46] Thus, the reduction in the percentage of aTregs might indeed be related to the IFN-γ-release and the pro-inflammatory shift in the TME caused by NK cells alone and, even more so, in combination with R848. In addition, a significant positive correlation between aTreg and $CD14^{hi}$ MoMC rates and a significant negative correlation between aTregs and $CD14^{neg}$ DC-like MoMC, underlines the importance of NK/myeloid crosstalk in the TME in tipping the balance in favor of a pro-inflammatory CD8 T cell/aTreg ratio. As IFN-γ is known to be involved in the NK-DC crosstalk[11] and able to assist DC-mediated Th1 responses,[51] it is likely that its production by NK cells is one of the mechanisms involved in NK cell-mediated inflammatory shift in the TME. In the current study we did not further delineate the mechanisms that directly drove the NK-myeloid crosstalk because of limited numbers of myeloid cells present in the samples. We did try to dissect these mechanisms in MoDC cultures. While CD154 and NKp30 were previously described to mediate the NK-MoDC crosstalk,[13 14] we could not establish a role for these receptors in our NK-MoDC crosstalk model (manuscript in preparation).

Although promising clinical outcomes have been achieved using adoptive NK cell therapy for the treatment of hematological malignancies, one of the challenges in a solid tumor setting is migration to the tumor site. Although we showed modest NK cell migration towards the supernatants of pCRC-SCS and mCRC-SCS cultures, previous studies demonstrated antitumor efficacy of the allogeneic NK cells against human solid tumors in an immunodeficient mouse model, clearly indicating the migration capabilities of NK cells.[6] Intraperitoneal infusion of NK cells in combination with R848 in patients with peritoneal metastases might circumvent this hurdle altogether. As patients with intraperitoneal carcinomatosis still represent a therapeutic challenge[43] intraperitoneal administration of NK cells, based on our findings, might present a highly needed novel treatment option.

Finally, this study assessed the impact of allogeneic NK cells on SCS, a two-dimensional model. However, to comprehensively elucidate these effects, follow-up investigations with a three-dimensional model are needed. One attractive option involves the usage of tissue slice cultures, which allow the preservation of the TME, including its immune components, for at least 5 days.[52]

In conclusion, our allogeneic off-the-shelf NK cells showed clear antitumor activity in both pCRC and mCRC cultures and induced a shift to a more pro-inflammatory state. This effect was enhanced by combining NK cells with the TLR7/8 ligand R848. Therefore, it would be of interest to study the combination of NK cells and R848 as a possible therapy for patients with (MSS-)CRC, aiming to achieve an improved and more effective T-cell response in the associated immunosuppressive TME, possibly leading to a systemic T-cell response and further supporting immune checkpoint blockade.

Author affiliations
[1]Department of Medical Oncology, Amsterdam UMC, Location Vrije Universiteit, Amsterdam, The Netherlands
[2]Cancer Center Amsterdam, Cancer Biology and Immunology, Amsterdam, The Netherlands
[3]Amsterdam Institute for Infection and Immunity, Amsterdam, The Netherlands
[4]Glycostem Therapeutics, Oss, The Netherlands
[5]Department of Molecular Cell Biology and Immunology, Amsterdam UMC, Location Vrije Universiteit, Amsterdam, The Netherlands
[6]Department of Medical Oncology, Erasmus MC University Medical Center, Rotterdam, The Netherlands
[7]Lava Therapeutics, Utrecht, The Netherlands
[8]Department of Surgery, Amsterdam UMC, Location Vrije Universiteit, Amsterdam, The Netherlands

Acknowledgements We thank all the patients who agreed to donate samples for this study and all the collaborators that supported the clinical sample collection, and Elisabetta Michielon for her help with the TGFβ ELISA.

Contributors TDdG, JS, ECT, AAvV and HJvdV conceived the study. TDdG, JS, HMWV and HJvdV supervised the project. ECT and AAvV performed experiments. JT provided patient samples. TDdG, JS, ECT, AAvV and HJvdV analyzed the data and prepared the figures. TDdG, JS, ECT, AAvV and HJvdV wrote the paper. TDdG is the guarantor of the study. All authors edited the manuscript and approved the final version. All authors have read and agreed to the published version of the manuscript.

Funding This work was funded by Glycostem Therapeutics BV.

Competing interests JS is chief scientific officer at Glycostem BV and HJvdV is chief scientific officer at Lava Therapeutics NV. TDdG is scientific advisor to Immunicum and Lava Therapeutics. AAvV is an employee of Glycostem BV.

Patient consent for publication Not applicable.

Ethics approval The material for this study was collected according to the guidelines of the Declaration of Helsinki of 1975 and under written informed consent. The pCRC samples were collected during an institutional review board-approved clinical trial of autologous whole-cell vaccination at the VU University medical center between 1987 and 1998. The mCRC samples were collected as part of the CRC biobank approved by the Medical Ethics Committee of the Vrije Universiteit Medisch Centrum (protocol code 109 2012/430, date of approval 2012) and by the Toetsingscommissie Biobank (protocol code 2018.27, date of approval 2017). Participants gave informed consent to participate in the study before taking part.

Provenance and peer review Not commissioned; externally peer reviewed.

Data availability statement Data are available upon reasonable request. The data that support the findings of this study are available from the corresponding author, TDdG, upon reasonable request.

ORCID iDs
Elisa C Toffoli http://orcid.org/0000-0003-0695-6479
Amanda A van Vliet http://orcid.org/0000-0001-6658-6575

REFERENCES

1 Xi Y, Xu P. Global colorectal cancer burden in 2020 and projections to 2040. *Transl Oncol* 2021;14:101174.
2 Ganesh K, Stadler ZK, Cercek A, *et al*. Immunotherapy in colorectal cancer: rationale, challenges and potential. *Nat Rev Gastroenterol Hepatol* 2019;16:361–75.
3 Vivier E, Tomasello E, Baratin M, *et al*. Functions of natural killer cells. *Nat Immunol* 2008;9:503–10.
4 Coca S, Perez-Piqueras J, Martinez D, *et al*. The prognostic significance of Intratumoral natural killer cells in patients with colorectal carcinoma. *Cancer* 1997;79:2320–8.
5 Tang Y-P, Xie M-Z, Li K-Z, *et al*. Prognostic value of peripheral blood natural killer cells in colorectal cancer. *BMC Gastroenterol* 2020;20:31.
6 Veluchamy JP, Lopez-Lastra S, Spanholtz J, *et al*. In vivo efficacy of umbilical cord blood stem cell-derived NK cells in the treatment of metastatic colorectal cancer. *Front Immunol* 2017;8:87.
7 Miller JS, Soignier Y, Panoskaltsis-Mortari A, *et al*. Successful adoptive transfer and in vivo expansion of human haploidentical NK cells in patients with cancer. *Blood* 2005;105:3051–7.
8 Dolstra H, Roeven MWH, Spanholtz J, *et al*. Successful transfer of umbilical cord blood CD34+ hematopoietic stem and progenitor-derived NK cells in older acute myeloid leukemia patients. *Clin Cancer Res* 2017;23:4107–18.
9 Velichinskii RA, Streltsova MA, Kust SA, *et al*. The biological role and therapeutic potential of NK cells in hematological and solid tumors. *Int J Mol Sci* 2021;22:11385.
10 Raes G, De Baetselier P, Van Ginderachter JA. Clinical and fundamental aspects of monocyte, macrophage and dendritic cell plasticity. *Eur J Immunol* 2012;42:13–6.
11 Ferlazzo G, Morandi B. Cross-talks between natural killer cells and distinct subsets of dendritic cells. *Front Immunol* 2014;5:159.
12 Böttcher JP, Bonavita E, Chakravarty P, *et al*. NK cells stimulate recruitment of CDc1 into the tumor microenvironment promoting cancer immune control. *Cell* 2018;172:1022–37.
13 Zhang AL, Colmenero P, Purath U, *et al*. Natural killer cells trigger differentiation of monocytes into dendritic cells. *Blood* 2007;110:2484–93.
14 Vitale M, Della Chiesa M, Carlomagno S, *et al*. NK-dependent DC maturation is mediated by TNFα and IFNγ released upon engagement of the NKp30 triggering receptor. *Blood* 2005;106:566–71.
15 Barry KC, Hsu J, Broz ML, *et al*. A natural killer–dendritic cell axis defines checkpoint therapy–responsive tumor microenvironments. *Nat Med* 2018;24:1178–91.
16 Gerhard GM, Bill R, Messemaker M, *et al*. Tumor-infiltrating dendritic cell States are conserved across solid human cancers. *J Exp Med* 2021;218:e20200264.
17 Lindenberg JJ, Fehres CM, van Cruijsen H, *et al*. Cross-talk between tumor and myeloid cells: how to tip the balance in favor of antitumor immunity. *Immunotherapy* 2011;3:77–96.
18 Bourdely P, Anselmi G, Vaivode K, *et al*. Transcriptional and functional analysis of CD1C+ human dendritic cells identifies a Cd163+ subset priming CD8+CD103+ T cells. *Immunity* 2020;53:335–352.
19 Smits ELJM, Ponsaerts P, Berneman ZN, *et al*. The use of TLR7 and TLR8 ligands for the enhancement of cancer immunotherapy. *Oncologist* 2008;13:859–75.
20 Adams S. Toll-like receptor agonists in cancer therapy. *Immunotherapy* 2009;1:949–64.
21 Saha T, van Vliet AA, Cui C, *et al*. Boosting natural killer cell therapies in glioblastoma multiforme using supramolecular cationic inhibitors of heat shock protein 90. *Front Mol Biosci* 2021;8:754443.
22 Vermorken JB, Claessen AM, van Tinteren H, *et al*. Active specific immunotherapy for stage II and stage III human colon cancer: a randomised trial. *Lancet* 1999;353:345–50.
23 Toffoli EC, Sheikhi A, Lameris R, *et al*. Enhancement of NK cell antitumor effector functions using a bispecific single domain antibody targeting CD16 and the epidermal growth factor receptor. *Cancers (Basel)* 2021;13:5446.
24 Dutertre C-A, Becht E, Irac SE, *et al*. Single-cell analysis of human mononuclear phagocytes reveals subset-defining markers and identifies circulating inflammatory dendritic cells. *Immunity* 2019;51:573–89.
25 van de Ven R, Lindenberg JJ, Oosterhoff D, *et al*. Dendritic cell plasticity in tumor-conditioned skin: CD14+ cells at the cross-roads of immune activation and suppression. *Front Immunol* 2013;4:403.
26 Miyara M, Yoshioka Y, Kitoh A, *et al*. Functional delineation and differentiation dynamics of human CD4+ T cells expressing the Foxp3 transcription factor. *Immunity* 2009;30:899–911.
27 Mannino MH, Zhu Z, Xiao H, *et al*. The paradoxical role of IL-10 in immunity and cancer. *Cancer Lett* 2015;367:103–7.
28 Kaplanski G. Interleukin-18: biological properties and role in disease pathogenesis. *Immunol Rev* 2018;281:138–53.
29 Han J, Khatwani N, Searles TG, *et al*. Memory CD8+ T cell responses to cancer. *Seminars in Immunology* 2020;49:101435.
30 Campbell KS, Hasegawa J. Natural killer cell biology: an update and future directions. *J Allergy Clin Immunol* 2013;132:536–44.
31 Spanholtz J, Tordoir M, Eissens D, *et al*. High log-scale expansion of functional human natural killer cells from umbilical cord blood CD34-positive cells for adoptive cancer Immunotherapy. *PLoS One* 2010;5:e9221.
32 Ferlazzo G, Tsang ML, Moretta L, *et al*. Human dendritic cells activate resting natural killer (NK) cells and are recognized via the NKp30 receptor by activated NK cells. *J Exp Med* 2002;195:343–51.
33 Roy S, Barnes PF, Garg A, *et al*. NK cells Lyse T regulatory cells that expand in response to an intracellular pathogen. *J Immunol* 2008;180:1729–36.
34 Josefowicz SZ, Rudensky A. Control of regulatory T cell lineage commitment and maintenance. *Immunity* 2009;30:616–25.
35 Chonov DC, Ignatova MMK, Ananiev JR, *et al*. IL-6 activities in the tumour microenvironment. Part 1. *Open Access Maced J Med Sci* 2019;7:2391–8.
36 Ma X, Yan W, Zheng H, *et al*. Regulation of IL-10 and IL-12 production and function in macrophages and dendritic cells. *F1000Res* 2015;4:F1000 Faculty Rev-1465.
37 Spranger S, Bao R, Gajewski TF. Melanoma-intrinsic β-Catenin signalling prevents anti-tumour immunity. *Nature* 2015;523:231–5.
38 Kistner L, Doll D, Holtorf A, *et al*. Interferon-inducible CXC-Chemokines are crucial immune Modulators and survival predictors in colorectal cancer. *Oncotarget* 2017;8:89998–90012.
39 Tokunaga R, Zhang W, Naseem M, *et al*. CXCL9, CXCL10, CXCL11/CXCR3 axis for immune activation - a target for novel cancer therapy. *Cancer Treat Rev* 2018;63:40–7.

40 Kadomoto S, Izumi K, Mizokami A. The CCL20-CCR6 axis in cancer progression. *Int J Mol Sci* 2020;21:5186.
41 Lupo KB, Matosevic S. Natural killer cells as allogeneic effectors in adoptive cancer immunotherapy. *Cancers (Basel)* 2019;11:769.
42 Guinney J, Dienstmann R, Wang X, *et al*. The consensus molecular subtypes of colorectal cancer. *Nat Med* 2015;21:1350–6.
43 Laoukili J, Constantinides A, Wassenaar ECE, *et al*. Peritoneal metastases from colorectal cancer belong to consensus molecular subtype 4 and are sensitised to oxaliplatin by inhibiting reducing capacity. *Br J Cancer* 2022;126:1824–33.
44 Lindenberg JJ, van de Ven R, Lougheed SM, *et al*. Functional characterization of a STAT3-de^{P}Endent Dendritic cell-derived CD14 + cell population arising upon IL-10-driven maturation. *Oncoimmunology* 2013;2:e23837.
45 Lindenberg JJ, Oosterhoff D, Sombroek CC, *et al*. IL-10 conditioning of human skin affects the distribution of migratory dendritic cell subsets and functional T cell differentiation. *PLoS One* 2013;8:e70237.
46 Lindenberg JJ, van de Ven R, Oosterhoff D, *et al*. Induction of dendritic cell maturation in the skin microenvironment by soluble factors derived from colon carcinoma. *Hum Vaccin Immunother* 2014;10:1622–32.
47 Fabbi M, Carbotti G, Ferrini S. Context-dependent role of IL-18 in cancer biology and counter-regulation by IL-18Bp. *J Leukoc Biol* 2015;97:665–75.
48 Josephs SF, Ichim TE, Prince SM, *et al*. Unleashing endogenous TNF-alpha as a cancer immunotherapeutic. *J Transl Med* 2018;16:242.
49 Swiecki M, Colonna M. Type I Interferons: diversity of sources, production pathways and effects on immune responses. *Curr Opin Virol* 2011;1:463–75.
50 Brillard E, Pallandre J-R, Chalmers D, *et al*. Natural killer cells prevent CD28-mediated Foxp3 transcription in CD4+CD25– T lymphocytes. *Exp Hematol* 2007;35:416–25.
51 Morandi B, Bougras G, Muller WA, *et al*. NK cells of human secondary lymphoid tissues enhance T cell polarizationvia IFN-Γ secretion. *Eur J Immunol* 2006;36:2394–400.
52 Kenerson HL, Sullivan KM, Labadie KP, *et al*. Protocol for tissue slice cultures from human solid tumors to study therapeutic response. *STAR Protoc* 2021;2:100574.

Table S1: Catalogue numbers and clones of used antibodies.

Antibodies	Fluorochrome	Brand	Catalog number	Clone
7AAD		Sigma	A9400-1MG	
BDCA-3	BV711	BD Biosciences	563155	1A4
CD103	BV711	Biolegend	334334	5C3
CD11c	APC-Cy7	Biolegend	337218	Bu15
CD14	FITC	BD Biosciences	345784	MΦP9
CD16	BV786	BD Biosciences	563690	3G8
CD1c	PE-Cy7	Sony	2257580	L161
CD25	APC	BD Biosciences	340907	2A3
CD25	FITC	BD Biosciences	345796	2A3
CD3	BV711	BD Biosciences	563725	UCHT1
CD3	PerCP-Cy5.5	BD Biosciences	332771	SK7
CD4	AF700	BD Biosciences	557922	RPA-T4
CD45	AF700	Biolegend	304024	HI30
CD45	PE-Cy7	BD Biosciences	557748	HI30
CD45RA	APC-H7	BD Biosciences	560674	HI100
CD56	BV510	BD Biosciences	563041	NCAM16.2
CD69	FITC	BD Biosciences	347823	L78
CD8	V500	BD Biosciences	561618	SK1
CD80	BV650	BD Biosciences	564158	L307.4
CD83	PE-CF594	BD Biosciences	562631	HB15e
CD86	PE	BD Biosciences	555658	2331(FUN-1)
CD88	BV711	BD Biosciences	742319	D53-1473
CD89	BV421	BD Biosciences	744374	A59
CTLA-4	PE-CF594	BD Biosciences	562742	BNI3
DNAM1	AF700	RnD Systems	FAB666N	102511
Epcam	BV421	BD Biosciences	563180	EBA-1

Epcam	FITC	Biolegend	324204	9C4
FoxP3	PE	eBioscience	12-4776-42	PCH101
HLA-ABC	PE	ThermoFisher	MA1-19662	W6/32
HLA-DR	APC	BD Biosciences	340907	2A3
HLA-E	PE	eBioscience	12-9953-42	3D12HLA-E
HLA-G	PE	Biolegend	335906	87G
KIR2D	FITC	Miltenyi Biotech	130-098-689	NKVFS1
Lag3	PE-Cy7	eBioscience	25-2239-42	3DS223H
MICA/B	PE	Biolegend	320906	6D4
Nectin-2	PE	Biolegend	337409	TX31
NKG2A	PE-Vio770	Miltenyi Biotech	130-114-093	REA110
NKG2C	PE	Miltenyi Biotech	130-119-776	REA205
NKG2D	APC	BD Biosciences	558071	1D11
NKp30	PE	Biolegend	325208	P30-15
NKp44	PE-Vio770	Miltenyi Biotech	130-120-356	REA1163
NKp46	APC	Miltenyi Biotech	130-092-609	9E2
PD-1	BV786	BD Biosciences	563789	EH12.1
PD-L1	BV786	BD Biosciences	563739	MIH1
PVR	PE	Biolegend	337610	SK11.4
Tim3	BV421	Biolegend	345008	F38-2E2
ULBP 1	PE	R&D systems	FAB1380P	170818
ULBP 2/5/6	PE	R&D systems	FAB1298P	165903
ULBP 3	PE	R&D systems	FAB1517P	166510

Table S2: Changes in NK cell receptor expression after 5 days upon co-culture of dissociated primary colorectal cancer samples in the presence and absence of sample and/or R848. NK cell:SCS ratio: 1:1. NK baseline is receptor expression of NK cells before co-culture. Abbreviations: T = tumor. R = R848. NK = NK cells

Marker	N	Conditions - Mean (SEM)				Analysis type	p-value	Multiple Comparison Analysis					
		NK baseline	NK	T + NK	T + NK + R848			NKbaseline-NK	NKbaseline –T+NK	NKbaseline - T+NK+R	NK-T+NK	NK-T+NK+R	T+NK - T+NK+R
%KIR2D	5	9.6 (2.0)	8.8 (1.6)	10.3 (1.6)	11.5 (1.5)	Friedman	ns	ns	ns	ns	ns	ns	ns
%NKG2A	5	56.6 (4.3)	64.3 (5.5)	66.2 (5.6)	68.5 (6.2)	ANOVA	**	ns	*	**	ns	ns	ns
%NKG2C	5	7.1 (1.0)	20.7 (4.1)	24.7 (4.7)	25.6 (3.6)	ANOVA	**	*	**	**	ns	ns	ns
%NKG2D	5	74.2 (5.0)	75.6 (3.8)	67.7 (6.2)	76.6 (6.7)	ANOVA	ns	ns	ns	ns	ns	ns	ns
%DNAM-1	5	68.4 (5.2)	78.9 (1.5)	78.3 (3.1)	79.6 (1.9)	ANOVA	ns	ns	ns	ns	ns	ns	ns
%CD25	5	6.0 (1.2)	34.0 (8.1)	33.9 (8.4)	41.5 (11.7)	ANOVA	**	*	*	**	ns	ns	ns
%NKp30	5	38.9 (10.7)	26.8 (6.9)	10.5 (5.4)	38.9 (10.7)	Friedman	ns	ns	ns	ns	ns	ns	ns
%NKp44	5	44.4 (6.4)	48.3 (5.9)	28.3 (12.3)	30.8 (13.6)	ANOVA	ns	ns	ns	ns	ns	ns	ns
%NKp46	5	76.1 (1.63)	86.2 (0.867)	85.7 (1.06)	86.4 (1.21)	Friedman	**	*	ns	ns	ns	ns	ns
%CD16	5	2.1 (0.3)	3.32 (0.4)	0.8 (0.6)	1.5 (0.6)	Friedman	ns	ns	ns	ns	ns	ns	ns

Table S3: Changes in NK cell receptor expression after 5 days upon co-culture of dissociated metastatic colorectal cancer samples in the presence and absence of sample and/or R848. NK cell:SCS ratio: 1:1. NK baseline is receptor expression of NK cells before co-culture Abbreviations: T = tumor. R = R848. NK = NK cells

Marker	N	Conditions - Mean (SEM)				Analysis type	p-value	Multiple Comparison Analysis					
		NK baseline	NK	T + NK	T + NK + R848			NKbaseline-NK	NKbaseline –T+NK	NKbaseline - T+NK+R	NK-T+NK	NK-T+NK+R	T+NK - T+NK+R
%KIR2D	6	6.6 (0.7)	4.2 (0.6)	6.3 (1.3)	6.3 (1.1)	Friedman	*	*	ns	ns	ns	ns	ns
%NKG2A	6	68.5 (5.2)	62.3 (2.2)	69.9 (3.6)	74.8 (2.6)	Friedman	*	ns	ns	ns	ns	*	ns
%NKG2C	6	6.4 (0.9)	15.8 (2.7)	13.3 (3.2)	12.2 (1.8)	Friedman	*	*	ns	ns	ns	ns	ns
%NKG2D	6	84.3 (3.3)	87.7 (2.0)	84.9 (1.7)	87.4 (1.2)	Friedman	ns	ns	ns	ns	ns	ns	ns
%DNAM-1	6	84.2 (4.4)	87.9 (2.4)	84.9 (2.2)	88 (2.1)	Friedman	ns	ns	ns	ns	ns	ns	ns
%CD25	6	2.7 (0.7)	19.9 (3.4)	19.8 (5.1)	25.5 (5.2)	Friedman	****	ns	ns	***	ns	ns	ns
%NKp30	6	13.2 (6.8)	6.0 (1.0)	5.6 (0.3)	5.3 (1.5)	Friedman	ns	ns	ns	ns	ns	ns	ns
%NKp44	6	78.9 (4.0)	17.2 (1.2)	28.4 (8.9)	30.7 (10.2)	ANOVA	****	****	***	***	ns	ns	ns
%NKp46	6	83.7 (1.99)	86.3 (1.76)	87.7 (1.01)	89.9 (0.920)	Friedman	*	ns	ns	*	ns	ns	ns
%CD16	6	12.0 (1.4)	6.0 (1.1)	10.5 (1.46)	9.7 (1.2)	Friedman	*	*	ns	ns	ns	ns	ns

Table S4: Changes in the myeloid and lymphocyte compartments and in the cytokine and chemokine concentrations upon culture of dissociated primary colorectal cancer samples in the presence and absence of NK cells and/or R848. NK cell:SCS ratio: 1:1. Abbreviations: T = tumor. R = R848. NK = NK cells.

Marker	N	Conditions - Mean (SEM)				Analysis type	p-value	Multiple Comparison Analysis					
		T	T+NK	T+R848	T+NK+R848			T – T+NK	T – T+R	T – T+R+NK	T+NK – T+R	T+NK – T+R+NK	T+R – T+R+NK
Myeloid Analysis Day 5													
% CD14 neg	9	16.9 (3.6)	28.3 (5.1)	30.8 (4.2)	48.2 (5.1)	ANOVA	****	**	****	****	ns	****	****
% CD14 dim	9	51.1 (7.4)	50.8 (5.3)	50.3 (5.0)	36.3 (4.9)	ANOVA	***	ns	ns	**	ns	**	**
% CD14 high	9	24.0 (6.1)	7.6 (2.8)	12.0 (3.4)	3.9 (1.7)	ANOVA	****	***	*	****	ns	ns	ns
CD14 neg CD80 MFI	9	19990 (5172)	20881 (5143)	22298 (5672)	32833 (6519)	ANOVA	****	ns	ns	***	ns	***	**
CD14 neg CD83 MFI	9	3691 (434.8)	4059 (457.3)	4715 (502.2)	6176 (692.8)	ANOVA	****	ns	ns	****	ns	***	*
CD14 neg CD86 MFI	4	10214 (3052)	10265 (2743)	15865 (2113)	29587 (4401)	ANOVA	**	ns	ns	**	ns	**	*
CD14 neg PD-L1 MFI	9	2609 (581)	2108 (355.5)	2186 (388.1)	2444 (491.7)	ANOVA	ns	ns	ns	ns	ns	ns	ns
CD14 neg Tim3 MFI	9	9802 (1813)	9108 (1687)	11231 (2369)	11961 (2152)	ANOVA	***	ns	ns	*	*	**	ns
CD14 neg BDCA3 MFI	9	6897 (1433)	5442 (970.9)	5944 (1087)	6211 (1068)	ANOVA	ns	ns	ns	ns	ns	ns	ns
Lymphocyte Analysis Day 5													
Ab. N. CD8⁺ T cells	4	238.7 (61.6)	232.2 (45.9)	213.5 (41.3)	196.4 (22.5)	ANOVA	ns	ns	ns	ns	ns	ns	ns
Ab. N. CD4⁺ T helper	4	679.6 (202.8)	601.7 (105.4)	640.3 (131.1)	533.4 (26.5)	ANOVA	ns	ns	ns	ns	ns	ns	ns
Absolut N aTreg	4	111.8 (34.0)	50.6 (12.3)	67.8 (15.8)	34.3 (12.2)	ANOVA	**	*	ns	**	ns	ns	ns
% aTreg	9	13.7 (1.8)	8.0 (1.3)	10.4 (1.7)	4.8 (1.1)	ANOVA	****	**	ns	****	ns	ns	**
CD8⁺ T cells %CD25	9	20.3 (3.5)	35.2 (5.2)	25.0 (3.6)	44.1 (4.9)	ANOVA	****	**	ns	****	ns	ns	***
CD8⁺ T cells %CD69	9	26.2 (6.1)	31.5 (6.0)	34.6 (7.1)	43.3 (5.9)	ANOVA	****	ns	*	****	ns	***	*
CD8⁺ T cells %CTLA4	9	15.9 (2.5)	12.2 (2.8)	14.9 (2.6)	16.0 (2.9)	ANOVA	ns	ns	ns	ns	ns	ns	ns

CD8⁺ T cells %PD-1	9	45.3 (7.6)	39.7 (7.6)	46.5 (7.9)	40.1 (8.0)	ANOVA	ns	ns	ns	ns	ns	ns	ns
CD8⁺ T cells %Tim3	9	13.6 (4.4)	26.0 (7.8)	16.7 (4.8)	31.9 (8.2)	Friedman	***	ns	ns	***	ns	ns	**
CD4⁺ T helper %CD25	9	18.6 (2.4)	28.7 (4.9)	22.3 (2.2)	30.9 (4.7)	ANOVA	**	*	ns	**	ns	ns	ns
CD4⁺ T helper %CD69	9	15.3 (2.6)	14.0 (3.5)	19.6 (3.4)	17.5 (3.8)	Friedman	***	ns	*	ns	***	*	ns
CD4⁺ T helper %CTLA4	9	43.6 (3.7)	35.2 (4.2)	41.4 (3.7)	36.9 (3.6)	ANOVA	ns	ns	ns	ns	ns	ns	ns
CD4⁺ T helper %Lag3	9	4.2 (1.4)	5.4 (1.5)	4.2 (1.1)	3.8 (0.6)	Friedman	ns	ns	ns	ns	ns	ns	ns
CD4⁺ T helper %PD-1	9	31.9 (6.1)	31.6 (5.3)	37.4 (6.2)	30.9 (5.5)	ANOVA	*	ns	ns	ns	ns	ns	ns
CD4⁺ T helper %Tim3	9	8.0 (2.6)	10.0 (3.6)	9.4 (2.5)	13.5 (4.7)	Friedman	ns	ns	ns	ns	ns	ns	ns
Cytokine Analysis Day 5 (pg/mL)													
IL-12p70	9	1.9 (0.6)	1.7 (0.5)	6.2 (2.4)	3.7 (1.7)	Friedman	***	ns	***	*	**	ns	ns
IFNα	9	2.6 (0.8)	4.6 (2.5)	51.7 (25.0)	79.7 (34.5)	Friedman	***	ns	ns	**	ns	**	ns
IL-10	9	47.3 (10.9)	21.2 (5.9)	109.1 (16.9)	58.1 (9.3)	Friedman	****	ns	ns	ns	****	*	ns
IL-6	9	38545 (6326)	21121 (5081)	42940 (6708)	14976 (3200)	Friedman	**	ns	ns	ns	ns	ns	*
IL-2	9	19.1 (4.0)	32.4 (7.6)	22.0 (6.8)	55.9 (10.5)	ANOVA	**	ns	ns	**	ns	ns	*
IFNγ	9	51 (21.12)	3495 (2005)	358.8 (122.1)	10342 (1775)	Friedman	****	*	ns	****	ns	ns	*
TNF	9	16.3 (5.5)	119.1 (62.6)	54.2 (14.8)	120.5 (26.9)	Friedman	***	ns	ns	***	ns	ns	ns
IL-15	9	3.2 (1.0)	8.1 (4.9)	3.8 (1.7)	8.2 (4.0)	Friedman	ns	ns	ns	ns	ns	ns	ns
IL-18	9	40.0 (11.4)	35.8 (6.09)	41.3 (9.0)	42.5 (8.5)	Friedman	ns	ns	ns	ns	ns	ns	ns
Chemokine Analysis Day 5 (pg/mL)													
CCL4	9	19.1 (4.5)	41.6 (12.2)	28.2 (5.8)	63.3 (16.4)	ANOVA	***	ns	ns	***	ns	**	ns
CCL5	9	84.0 (13.5)	254.7 (66.1)	164.9 (38.2)	530.1 (137.1)	Friedman	****	*	ns	****	ns	ns	*

CXCL9	9	124.7 (45.3)	308.9 (147.9)	189.4 (52.7)	302.9 (138.4)	Friedman	ns	ns	ns	ns	ns	ns	ns
CXCL10	9	650.4 (236.9)	332.0 (56.6)	1763.4 (669.9)	755.1 (156.6)	Friedman	*	ns	ns	ns	*	ns	ns
CXCL11	9	5.6 (2.3)	2.6 (0.7)	8.5 (3.9)	3.3 (0.6)	Friedman	*	ns	ns	ns	ns	ns	ns
CCL20	9	40.7 (11.5)	17.6 (6.0)	23.4 (5.6)	13.0 (6.3)	Friedman	*	ns	ns	*	ns	ns	ns

Table S5: Changes in the myeloid and lymphocyte compartments and in the cytokine and chemokine concentrations upon culture of dissociated metastatic colorectal cancer samples in the presence and absence of NK cells and/or R848. NK cell:SCS ratio: 1:1. Abbreviations: T = tumor. R = R848. NK = NK cells.

Marker	N	Conditions				Analysis type	p-value	Multiple Comparison Analysis					
		T	T+NK	T+R848	T+NK+R848			T – T+NK	T – T+R	T – T+R+NK	T+NK – T+R	T+NK – T+R+NK	T+R – T+R+NK
Myeloid Analysis Day 5													
% CD14 neg	6	7.7 (0.9)	21.8 (5.2)	17.6 (3.3)	27.9 (5.2)	ANOVA	***	**	ns	***	ns	ns	ns
% CD14 dim	6	17.7 (1.3)	47.3 (5.6)	35.1 (5.7)	37.1 (4.1)	ANOVA	**	***	*	*	ns	ns	ns
% CD14 high	6	74.1 (1.3)	29.3 (10.2)	46.4 (7.5)	33.4 (8.4)	ANOVA	***	***	*	**	ns	ns	ns
CD14 neg CD80 MFI	6	57217 (11402)	49960 (11464)	21954 (4030)	40163 (16987)	Friedman	ns	ns	ns	ns	ns	ns	ns
CD14 neg CD83 MFI	6	7945 (898.6)	7896 (1258)	6538 (1117)	6239 (1338)	Friedman	ns	ns	ns	ns	ns	ns	ns
CD14 neg CD86 MFI	6	35604 (21419)	33465 (21824)	9900 (1338)	16316 (8341)	Friedman	ns	ns	ns	ns	ns	ns	ns
CD14 neg PD-L1 MFI	6	7119 (668.2)	8797 (1570)	7429 (1129)	5127 (1319)	Friedman	ns	ns	ns	ns	ns	ns	ns
CD14 neg Tim3 MFI	6	17786 (825.6)	19517 (1856)	16339 (811.7)	16990 (1911)	ANOVA	ns	ns	ns	ns	ns	ns	ns
CD14 neg BDCA3 MFI	6	7575 (1666)	5809 (1598)	4230 (827.8)	3398 (674.9)	ANOVA	**	ns	ns	*	ns	ns	ns
Lymphocyte Analysis Day 5													
Ab. N. CD8⁺ T cells	6	1028 (174.9)	1225 (314.1)	1323 (373.5)	1211 (387.3)	ANOVA	ns	ns	ns	ns	ns	ns	ns
Ab. N. CD4⁺ T helper	6	1944 (438)	2246 (577.4)	2467 (894.9)	2526 (1206)	Friedman	ns	ns	ns	ns	ns	ns	ns
Absolut N aTreg	6	121 (38.3)	78.7 (22.9)	58.6 (18.3)	29.0 (6.3)	ANOVA	ns	ns	ns	*	ns	ns	ns
% aTreg	7	5.9 (1.2)	2.9 (0.5)	3.5 (1.1)	1.5 (0.3)	ANOVA	**	*	ns	**	ns	ns	ns
CD8⁺ T cells %CD25	7	8.8 (2.8)	18.8 (3.3)	10.0 (2.5)	27.4 (5.3)	ANOVA	***	ns	ns	***	ns	ns	***
CD8⁺ T cells %CD69	7	14.4 (3.9)	15.2 (3.1)	19.9 (5.5)	18.7 (3.1)	ANOVA	ns	ns	ns	ns	ns	ns	ns

CD8⁺ T cells %CTLA4	7	16.1 (2.4)	12.3 (3.0)	18.7 (3.5)	16.5 (3.8)	ANOVA	*	ns	ns	ns	*	ns	ns
CD8⁺ T cells %PD-1	7	27.0 (8.2)	27.3 (8.4)	28.0 (8.4)	27.9 (7.2)	ANOVA	ns	ns	ns	ns	ns	ns	ns
CD8⁺ T cells %Tim3	7	5.6 (1.3)	10.8 (3.6)	9.9 (3.6)	11.5 (5.1)	Friedman	ns	ns	ns	ns	ns	ns	ns
CD4⁺ T helper %CD25	7	7.7 (1.1)	24.5 (7.1)	11.2 (1.9)	30.8 (9.0)	Friedman	***	ns	ns	***	ns	ns	*
CD4⁺ T helper %CD69	7	16.3 (2.9)	16.0 (4.0)	17.7 (4.6)	16.2 (2.9)	ANOVA	ns	ns	ns	ns	ns	ns	ns
CD4⁺ T helper %CTLA4	7	40.8 (5.3)	30.7 (5.4)	42.8 (5.6)	35.4 (6.6)	ANOVA	***	**	ns	ns	***	ns	*
CD4⁺ T helper %PD-1	7	31.4 (7.6)	30.1 (8.3)	28.5 (7.6)	26.3 (6.8)	ANOVA	ns	ns	ns	ns	ns	ns	ns
CD4⁺ T helper %Tim3	7	7.7 (3.2)	16.6 (7.5)	10.5 (4.6)	19.7 (9.3)	Friedman	ns	ns	ns	ns	ns	ns	ns
Cytokine Analysis Day 5 (pg/mL)													
IL-12p70	6	0.5 (0.005)	0.6 (0.04)	1.6 (0.1)	0.9 (0.1)	Friedman	****	ns	***	ns	ns	ns	ns
IFNα	6	0.5 (0.04)	0.8 (0.2)	9.1 (4.3)	5.05 (2.9	Friedman	***	ns	*	*	ns	ns	ns
IL-10	6	205 (78.6)	36.3 (14.4)	1573.2 (413.0)	609.8 (234.7)	Friedman	****	ns	ns	ns	***	*	ns
IL-6	6	87230 (12801)	10278 (6135)	98956 (13835)	7887 (2534)	Friedman	***	ns	ns	*	ns	ns	*
IL-2	6	11.23 (2.52)	33.38 (4.162)	29.52 (3.117)	59 (3.716)	ANOVA	****	**	**	****	ns	***	***
IFNγ	6	7.992 (3.748)	1834 (636.8)	433.9 (145.6)	13067 (841.4)	Friedman	****	*	ns	***	ns	ns	*
TNF	6	17.29 (7.94)	111.1 (18.87)	2488 (987.5)	1342 (513.4)	Friedman	****	ns	***	*	ns	ns	ns
IL-15	6	4.358 (0.04833)	43 (13.46)	5.322 (0.4977)	43.62 (12.02)	Friedman	**	*	ns	ns	ns	ns	ns
IL-18	6	142.9 (40.95)	108.3 (44.84)	296 (105.7)	252.4 (96.35)	Friedman	**	ns	ns	ns	*	*	ns
Chemokine Analysis Day 5 (pg/mL)													
CCL4	6	12.0 (3.0)	31.8 (7.6)	93.7 (30.1)	82.9 (17.0)	ANOVA	**	ns	*	*	ns	ns	ns

CCL5	6	47.9 (18.7)	133.6 (31.2)	424.4 (253.6)	504.6 (163.1)	Friedman	***	ns	ns	**	ns	ns	ns
CXCL9	6	70.1 (35.8)	569.5 (90.9)	384.8 (110.8)	465 (138.4)	Friedman	**	*	ns	ns	ns	ns	ns
CXCL10	6	217.8 (129)	1453 (661)	2002 (1237)	1939 (1171)	Friedman	*	ns	*	ns	ns	ns	ns
CXCL11	6	1.2 (0.4)	3.2 (0.9)	8.4 (5.1)	6.3 (3.6)	Friedman	ns	ns	ns	ns	ns	ns	ns
CCL20	6	640.5 (347.7)	89.8 (56.1)	1011 (470.5)	125 (83.1)	Friedman	****	ns	ns	ns	**	ns	*

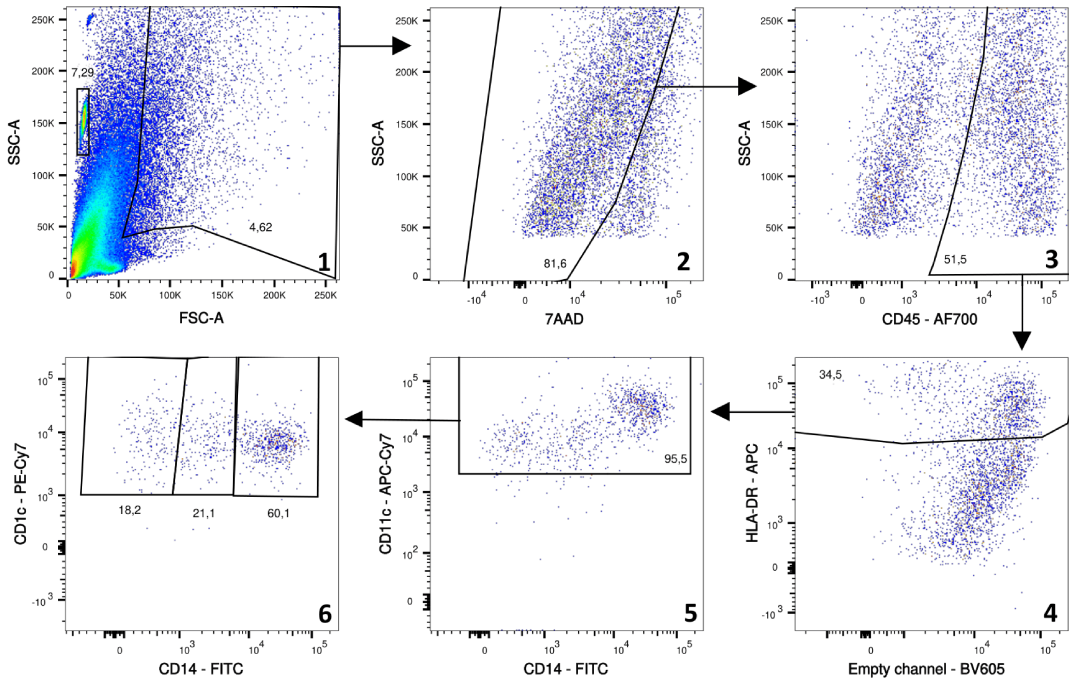

Figure S1: *Example of myeloid gating strategy. Percentages of the gated populations are listed in the plots.*

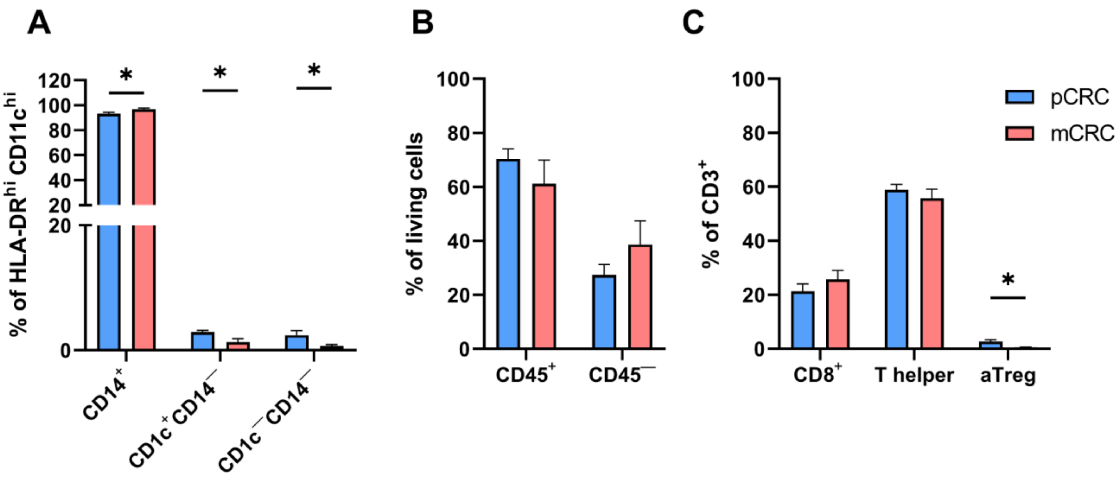

Figure S2: *Baseline characterization of the tumor microenvironment.* Differences between pCRC and mCRC in the myeloid subsets defined by the expression of (**A**) CD14 and CD1c (**B)** in the percentages of CD45^{+} and CD45^{-} cells and in **C)** the distribution of CD8^{+}, T helper and aTreg. pCRC: *n* = 9. mCRC: *n* = 5. The data are presented as mean ± SEM. Significance is presented as p <0.05 *. p-values were determined by Mann-Whitney test (**A, C**) or two-tailed T-test (**B**). Abbreviations: pCRC = primary colorectal cancer, mCRC = metastatic colorectal cancer, aTreg = activated regulatory T cells.

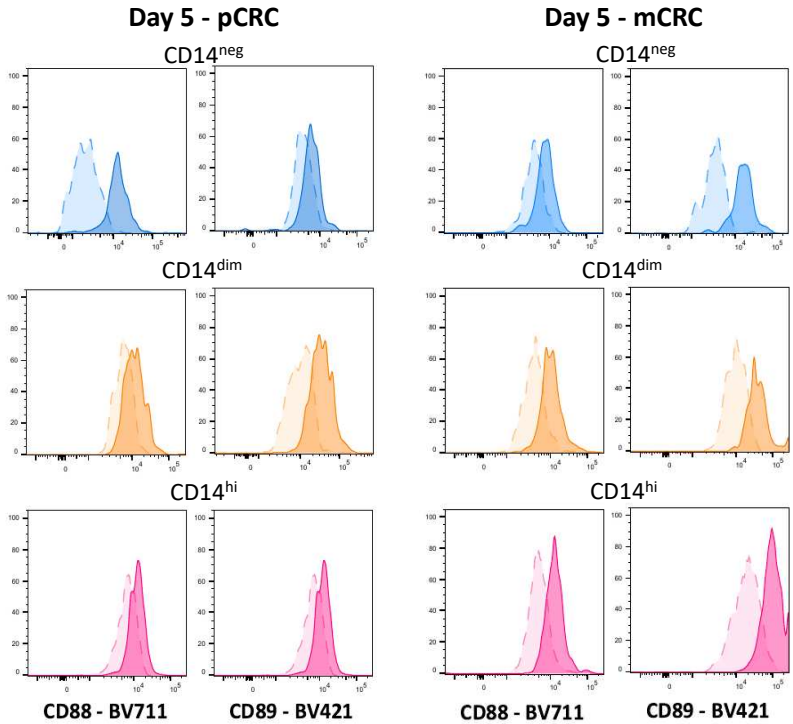

Figure S3: *Expression of CD88 and CD89 on the different myeloid subsets defined by the expression of CD14 (CD14^{neg}, CD14^{dim}, CD14^{hi}) after 5-day culture.* Concatenated data; pCRC: *n* = 4, mCRC: *n* = 6. Darker color: stained; lighter color: FMO. Abbreviations: pCRC = primary colorectal cancer, mCRC = metastatic colorectal cancer.

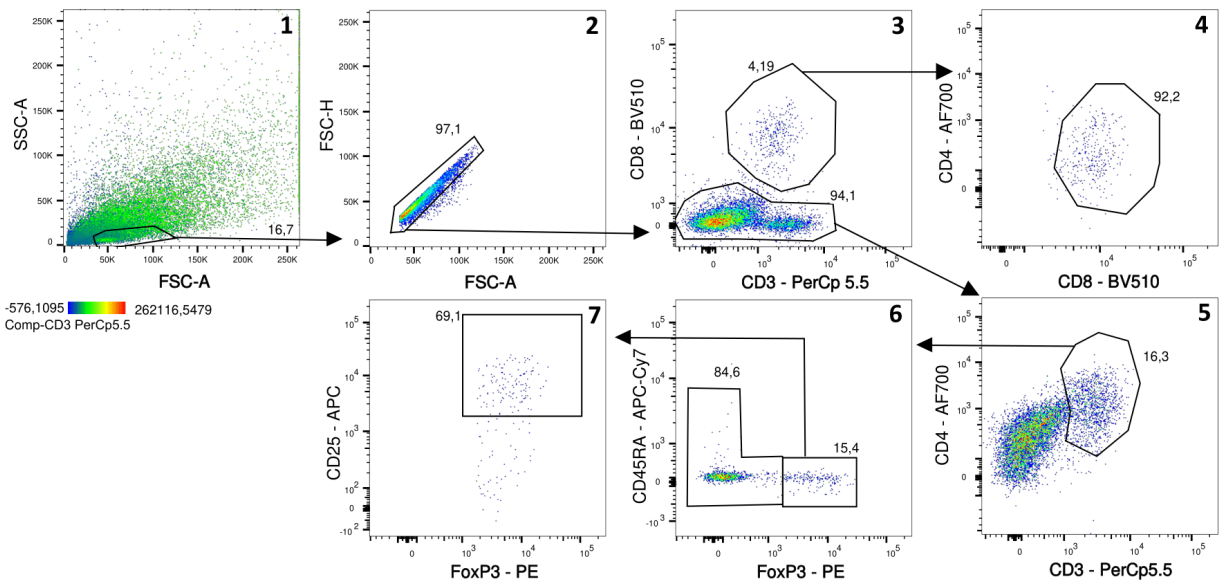

Figure S4: *Example of T cell gating strategy*. Perventages of gated cells are shown in the plots.

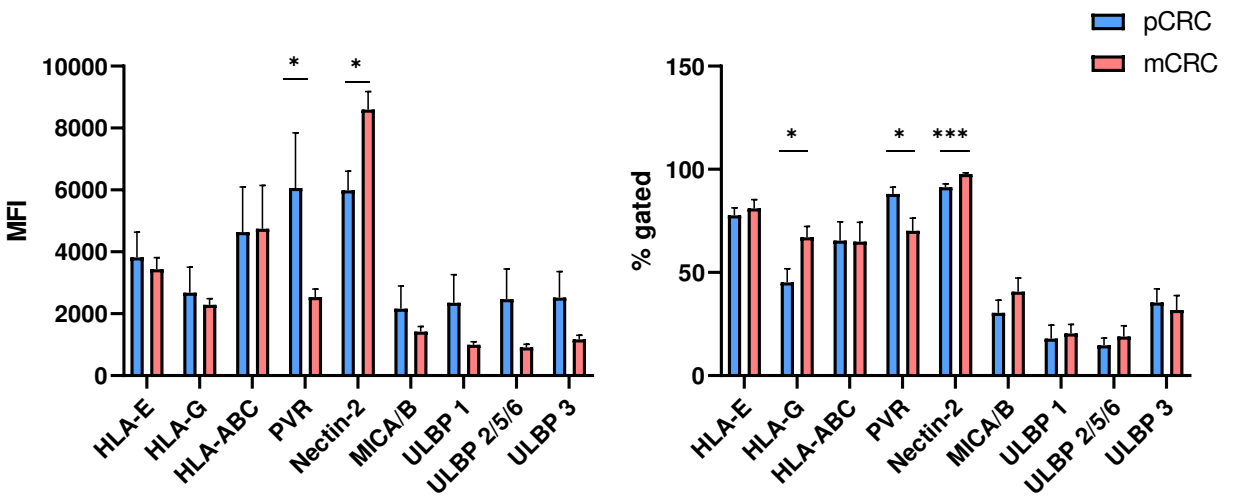

Figure S5: *Expression of NK cell ligands on the surface of CRC tumor cells, defined as Epcam⁺CD45⁻.* The data are presented as median fluorescence intensity (MFI) and percentage of positive cells. pCRC *n* = 12 (HLA-ABC *n* = 10), mCRC *n* = 12 (Nectin-2 *n* = 7). The data are presented as mean ± SEM. Significance is presented as *p* <0.05 *, <0.01 **, 0.001 ***. *p*-values are determined by Mann-Whitney test.

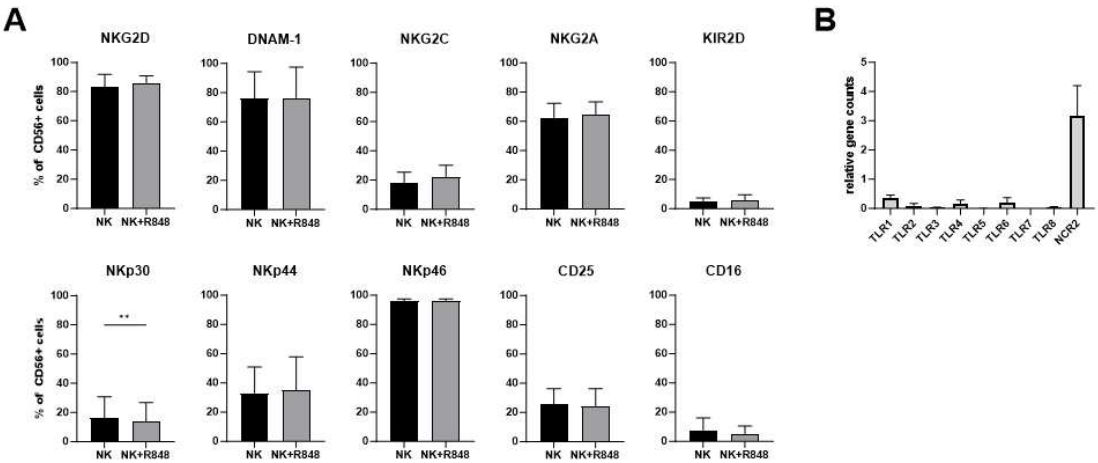

Figure S6: *Effect of R848 on NK phenotype and TLR expression on NK cells.* (**A**) Receptor expression (in percentages) at day 5 of NK cells alone or in co-culture with R848 (*n*=6). Significance is presented as <0.01 **. *p*-values were determined by two-tailed paired T-test analysis. (**B**) TLR expression obtained via whole transcriptome RNA sequencing, represented as relative gene counts. Relative gene count is calculated as ratio of the average count per gene based on 18647 analyzed genes. NCR2 (NKp44) is added as control of a gene that is highly expressed and with a similar gene size (*n*=9).

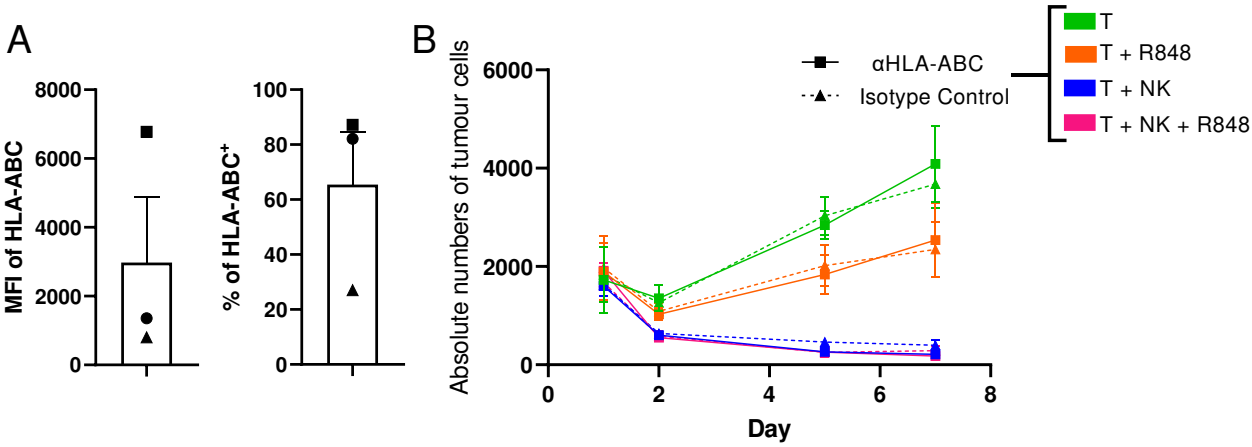

Figure S7: *Effect of NK cells and CD8⁺ T cells on tumor growth control*. (**A**) Expression of HLA-ABC on Epcam⁺CD45⁻ cells. The data are presented as median fluorescence intensity or percentage of positive cells. The symbols correspond to the different dissociated tumor samples used in the cytotoxicity assay (**B**). *n* = 3. (**B**) Cytotoxicity assay performed by co-culturing dissociated pCRC tissue in the presence and absence of NK cells, R848 and either HLA-ABC blocking antibodies (10 ug/mL, Thermofisher, cat: MA1-19027) or an IgG2a isotype control (10 ug/mL, Biolegend, cat: 401504) for 1,2,5 and 7 days. The readout is based on the absolute numbers of alive tumor cells (Epcam⁺CD45⁻7AAD⁻) quantified with QUANTI BEADS (Invitrogen, Thermo Fisher Scientific). NK cell:SCS ratio: 1:1. *n* = 3; 2 NK donors. The data are presented as mean ± SEM. *p*-values are determined by two-way ANOVA with Tukey's multiple comparisons analysis (**B**). Abbreviations: T = tumor, NK = NK cells.

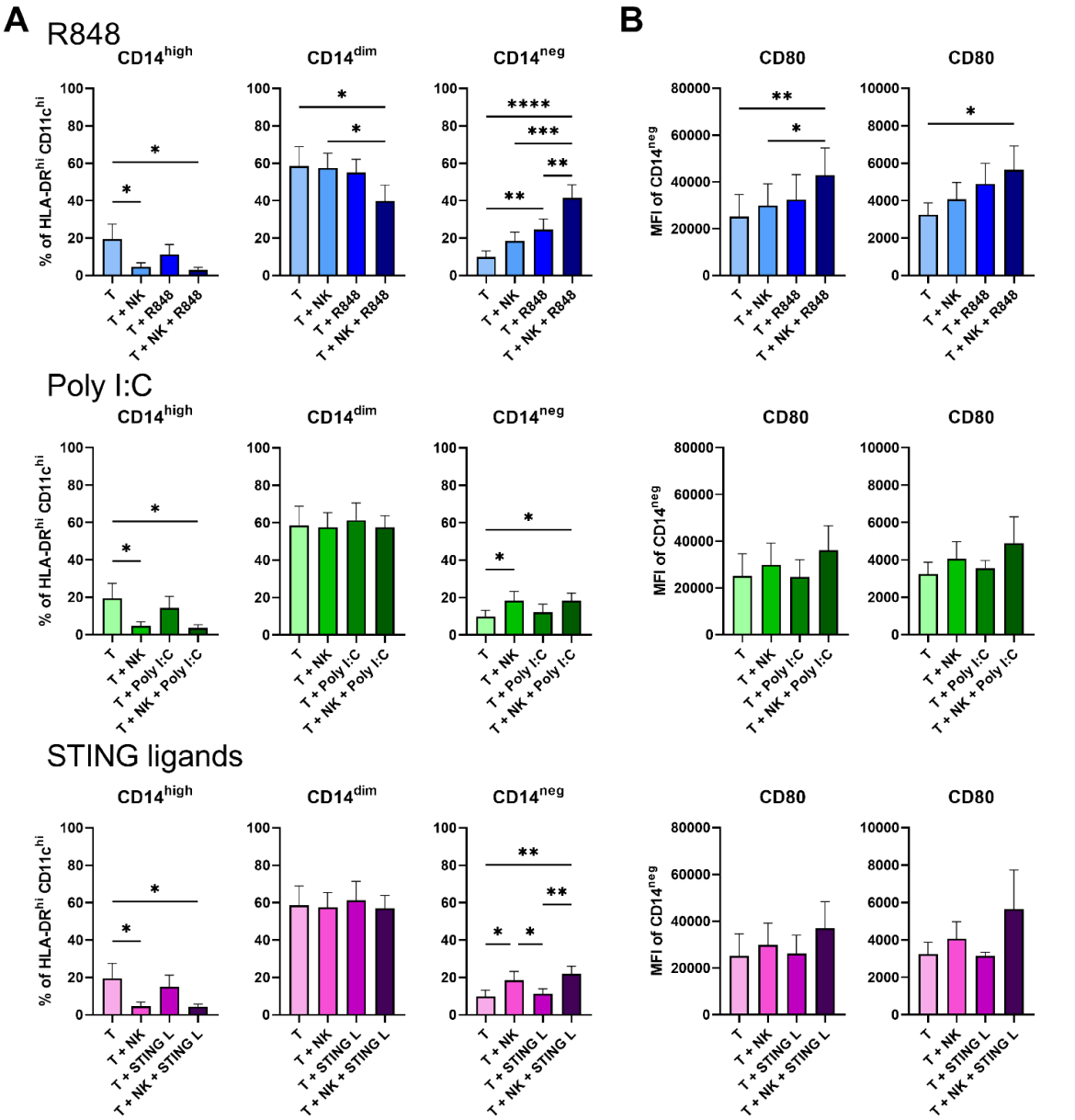

Figure S8: *The combination of NK cells with R848 induces a stronger monocyte-to-dendritic cell conversion and CD80 and CD80 upregulation on CD14^{neg} MoMC compared the combination of the NK cells with Poly IC or STING ligands after a 5-day co-culture with pCRC-SCS.*

(**A**) Changes in the percentages of CD14^{hi}, CD14^{dim}, CD14^{neg} (n=5) and (**B**) in the expression level (in Mean Fluorescence Intensity [MFI]) of CD80 and CD83 on CD14^{neg} cells (pCRC: *n*=4; 2 NK donors). Poly I:C (20 µL/mL, Invivogen, SanDiego CA). STING ligand (cyclic-di-AMP and rr-cyclic-di-AMP, 10 µL/mL Invivogen, San Diego CA). The data are presented as mean ± SEM. Significance is presented as *p* <0.05 *, <0.01 **, 0.001 ***, 0.0001 ****. *p*-values are determined by one-way ANOVA with Tukey multiple comparison analysis. Abbreviations: pCRC = primary colorectal cancer, T = tumor, NK = NK cells, STING L: STING ligands.

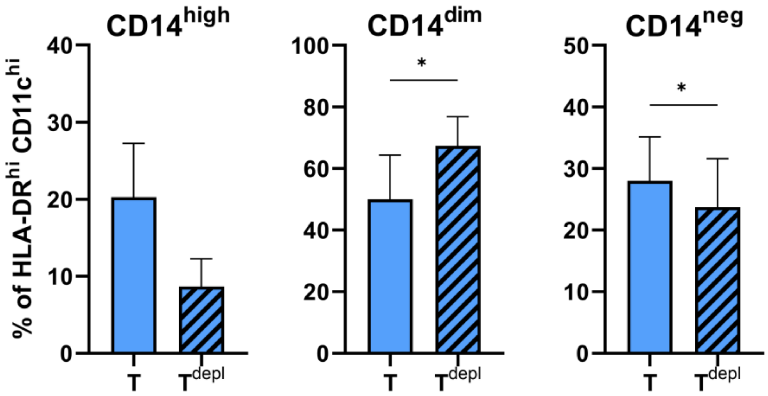

Figure S9: *Effects of tumor cell depletion on the myeloid compartment of dissociated pCRC samples.* Changes in the percentages of $CD14^{high}$, $CD14^{dim}$, $CD14^{neg}$ monocyte-derived myeloid cells after 5-day culture of dissociated pCRC or tumor-depleted dissociated pCRC samples. The myeloid cells were defined as $CD45^{+}HLA\text{-}DR^{high}CD11c^{high}$. *n* = 3; 2 NK donors. The data are presented as mean ± SEM. Significance is presented as $p < 0.05$ *. *p*-values are determined by two-tailed paired T-test. Abbreviations: T = tumor, T^{depl}: tumor depleted.

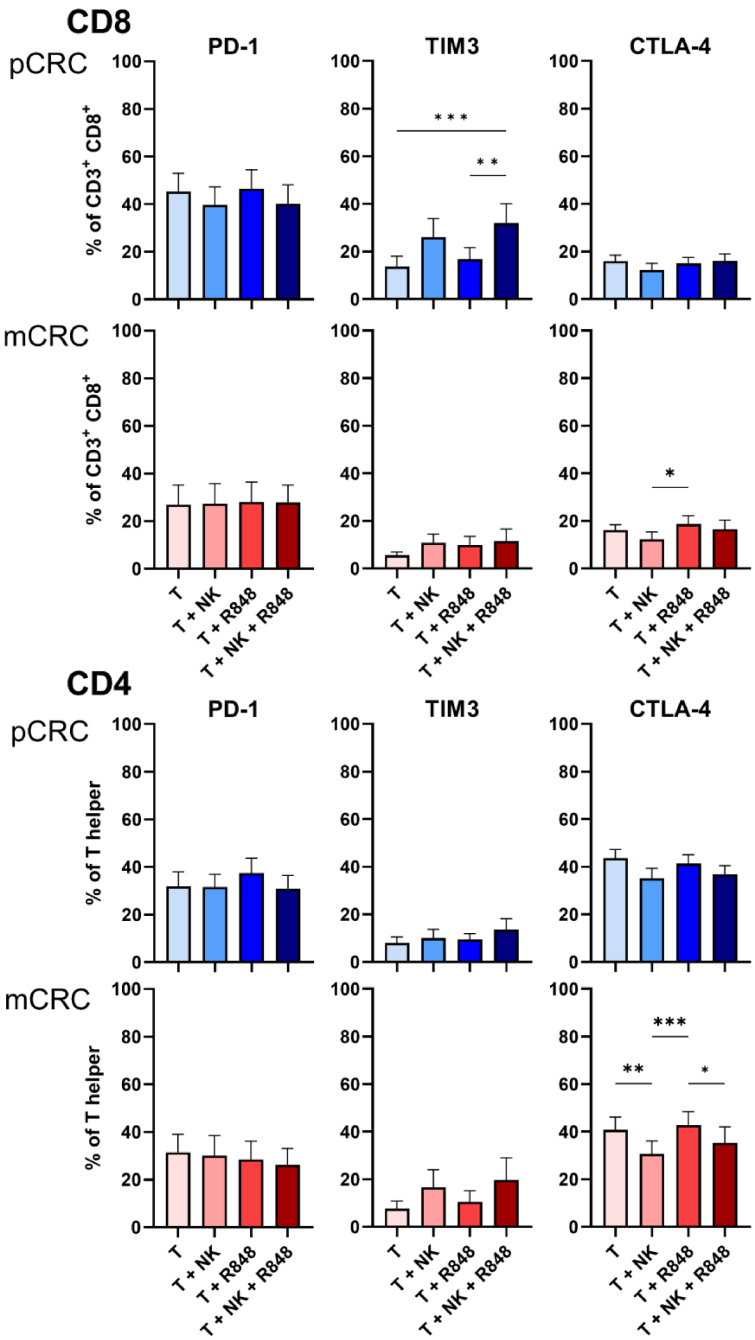

Figure S10: *Changes in the expression of immune checkpoints on CD8⁺ T cells and CD4⁺ T helper cells after 5-day culture of dissociated pCRC or mCRC samples in the presence and absence of NK cells and/or R848*. NK cell:SCS ratio: 1:1. pCRC: n = 9; 3 NK donors. mCRC: n = 7; 3 NK donors. The data are presented as mean ± SEM. *p*-values are determined by one-way ANOVA with Tukey multiple comparison analysis or Friedman test with Dunn multiple comparison analysis (pCRC and mCRC: TIM3). Abbreviations: pCRC = primary colorectal cancer, mCRC = metastatic colorectal cancer, T = tumor, NK = NK cells.

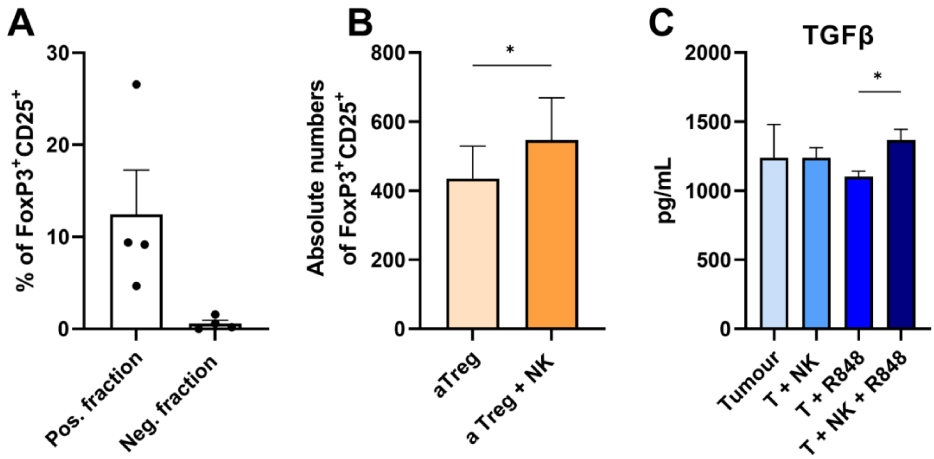

Figure S11: *Effect of NK cells on aTreg.* (**A**) Enrichement of aTreg (defined as FoxP3$^+$CD25$^+$CD45RA$^-$) of dissociated pCRC samples executed by performing multiple magnetic bead-activated cell sorting (MACS). First the tumor cells were depleted using CD326 (EpCAM) MicroBeads (Miltenyi Biotech, cat: 130-061-101). Next, CD4$^+$ T cells were isolated with CD4$^+$ T cell isolation kit (Miltenyi Biotech, cat: 130-096-533). Finally, CD25$^+$ CD4$^+$ T cells were isolated using CD25 Microbeads II (Miltenyi Biotech, cat: 130-092-983). All the MACS kit were used according to manufacturer's instructions. *n* = 4. (**B**) Absolute number of FoxP3$^+$CD25$^+$CD45RA$^-$ cells after 24h culture of aTreg enriched dissociated pCRC and NK cells. NK cell:SCS ratio 1:1. *n* = 3 pCRC and 2 NK donors. (**C**) TGFβ levels in the supernatant of dissociated pCRC samples cultured for 5 days in the presence and absence of NK cells and/or R848, determined with the TGF-β1 ELISA kit (R&D, cat: DY240). NK cell:SCS ratio: 1:1. *n* = 4. Significance is presented as p <0.05 *. p-values are determined by two-tailed paired T test (B) or one-way ANOVA with Tukey multiple comparison analysis (C). Abbreviations: T = tumor, aTreg = activated regulatory T cells, NK = NK cells, aTreg = activated regulatory T cells.

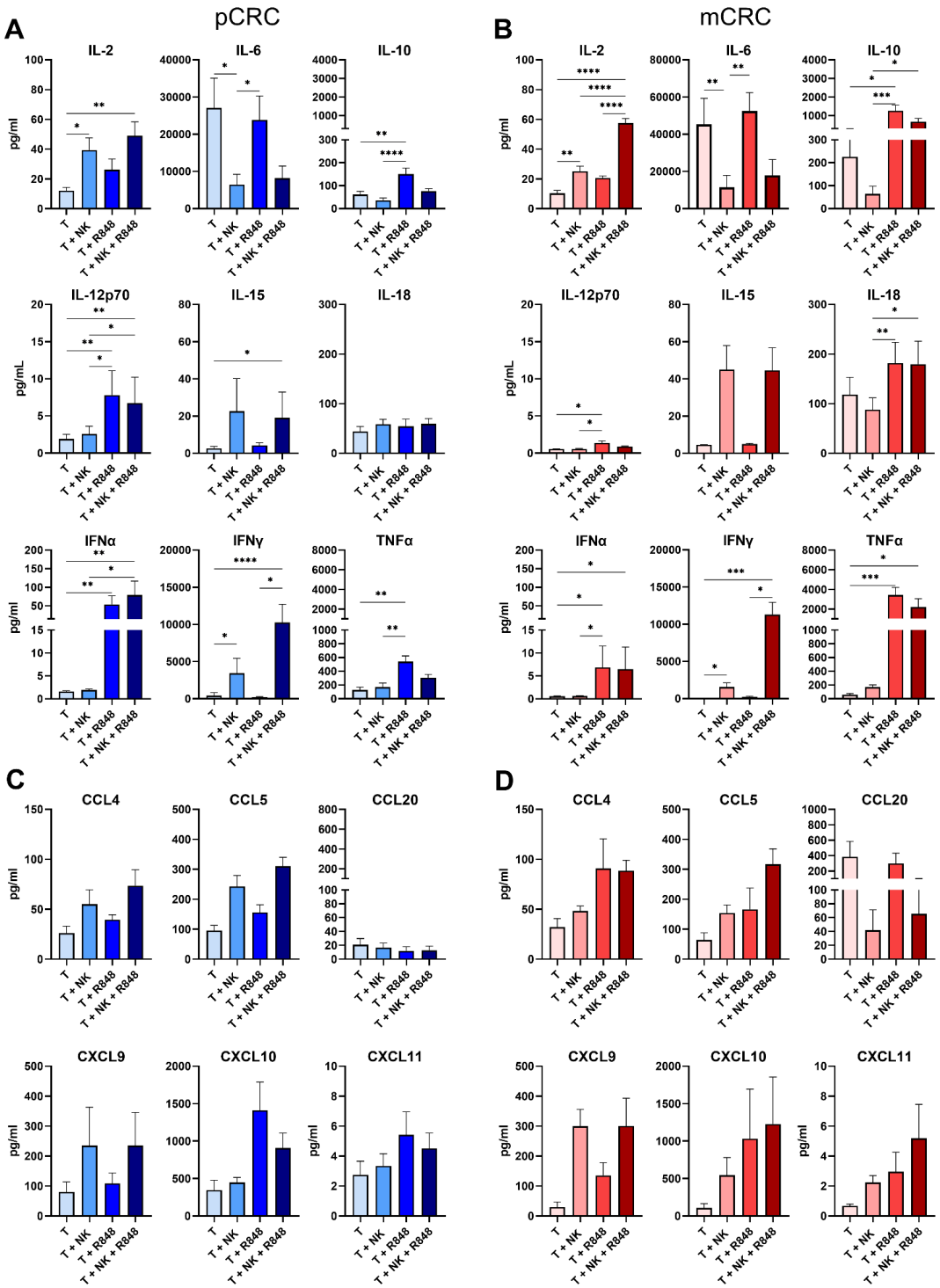

Figure S12 *Changes in the cytokine and chemokine profile upon a 2 day co-culture of pCRC- or mCRC-SCS with or without NK cells and/or R848*. Cytometry Bead Array performed on the supernatant of pCRC- or mCRC-SCS cultured for 2 days in the presence and absence of NK cells and/or R848. NK cell:SCS ratio 1:1. Cytokine levels: (**A**) pCRC- and (**B**) mCRC-SCS. Chemokine levels: (**C**) pCRC- and (**D**) mCRC-SCS. PCRC: *n* = 9; 3 NK donors (IL-6 *n* = 5), mCRC: *n* = 6; 3 NK donors. The data are presented as mean ± SEM. Significance is presented as *p* <0.05 *, <0.01 **, 0.001 ***, 0.0001 ****. *p*-values are determined by Friedman ANOVA with Dunn multiple comparison analysis or one-way ANOVA with Tukey multiple comparison analysis (pCRC: IL-2, CCL4, CCL5; mCRC: IL-2, CCL4). Abbreviations: pCRC = primary colorectal cancer, mCRC = metastatic colorectal cancer, T = tumor, NK = NK cells.